AD-A133 240 A DESIGN FOR A TEST BED SCOUR JET ARRAY FOR MARE ISLAND 1/1
NAVAL SHIPYARD(U) NAVAL CIVIL ENGINEERING LAB PORT
HUENEME CA J A BAILARD ET AL. MAY 83 NCEL-TR-899

UNCLASSIFIED F/G 13/2 NL

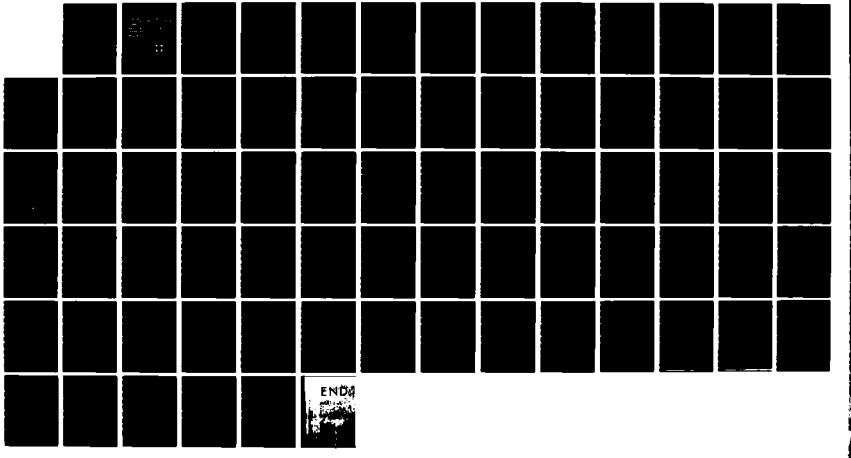

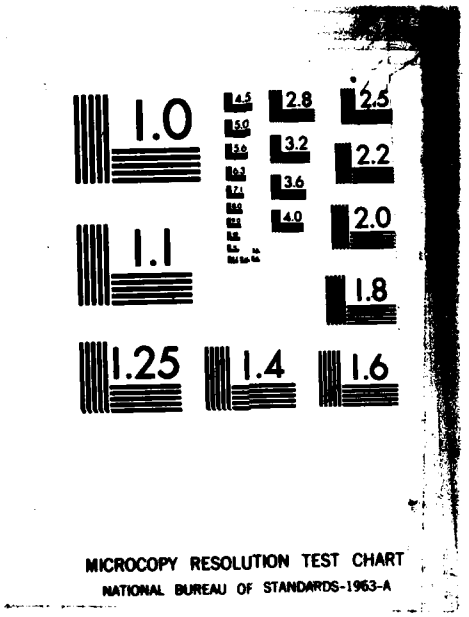

A Design for a Test Bed Scour Jet Array for Mare Island Naval Shipyard

By J. A. Bailard and J. M. Camperman

May 1983

Technical Report R-899
Naval Civil Engineering Laboratory
Port Hueneme, California 93043

Sponsored by the Naval Facilities Engineering Command

METRIC CONVERSION FACTORS

Approximate Conversions to Metric Measures

Symbol	When You Know	Multiply by	To Find	Symbol
		LENGTH		
in	inches	*2.5	centimeters	cm
ft	feet	30	centimeters	cm
yd	yards	0.9	meters	m
mi	miles	1.6	kilometers	km
		AREA		
in^2	square inches	6.5	square centimeters	cm^2
ft^2	square feet	0.09	square meters	m^2
yd^2	square yards	0.8	square meters	m^2
mi^2	square miles	2.6	square kilometers	km^2
	acres	0.4	hectares	ha
		MASS (weight)		
oz	ounces	28	grams	g
lb	pounds	0.45	kilograms	kg
	short tons (2,000 lb)	0.9	tonnes	t
		VOLUME		
tsp	teaspoons	5	milliliters	ml
Tbsp	tablespoons	15	milliliters	ml
fl oz	fluid ounces	30	milliliters	ml
c	cups	0.24	liters	l
pt	pints	0.47	liters	l
qt	quarts	0.95	liters	l
gal	gallons	3.8	liters	l
ft^3	cubic feet	0.03	cubic meters	m^3
yd^3	cubic yards	0.76	cubic meters	m^3
		TEMPERATURE (exact)		
°F	Fahrenheit temperature	5/9 (after subtracting 32)	Celsius temperature	°C

*1 in = 2.54 (exactly). For other exact conversions and more detailed tables, see NBS Misc. Publ. 286, Units of Weights and Measures, Price $2.25, SD Catalog No. C13.10:286.

Approximate Conversions from Metric Measures

Symbol	When You Know	Multiply by	To Find	Symbol
		LENGTH		
mm	millimeters	0.04	inches	in
cm	centimeters	0.4	inches	in
m	meters	3.3	feet	ft
m	meters	1.1	yards	yd
km	kilometers	0.6	miles	mi
		AREA		
cm^2	square centimeters	0.16	square inches	in^2
m^2	square meters	1.2	square yards	yd^2
km^2	square kilometers	0.4	square miles	mi^2
ha	hectares (10,000 m^2)	2.5	acres	
		MASS (weight)		
g	grams	0.035	ounces	oz
kg	kilograms	2.2	pounds	lb
t	tonnes (1,000 kg)	1.1	short tons	
		VOLUME		
ml	milliliters	0.03	fluid ounces	fl oz
l	liters	2.1	pints	pt
l	liters	1.06	quarts	qt
l	liters	0.26	gallons	gal
m^3	cubic meters	35	cubic feet	ft^3
m^3	cubic meters	1.3	cubic yards	yd^3
		TEMPERATURE (exact)		
°C	Celsius temperature	9/5 (then add 32)	Fahrenheit temperature	°F

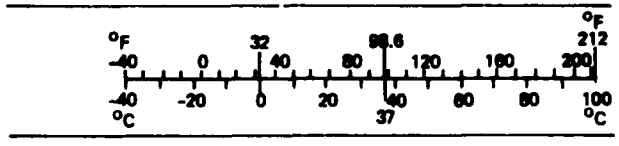

Unclassified

SECURITY CLASSIFICATION OF THIS PAGE (When Data Entered)

REPORT DOCUMENTATION PAGE		READ INSTRUCTIONS BEFORE COMPLETING FORM
1 REPORT NUMBER TR-899	2 GOVT ACCESSION NO DN987047	3 RECIPIENT'S CATALOG NUMBER AD-A133240
4 TITLE (and Subtitle) A DESIGN FOR A TEST BED SCOUR JET ARRAY FOR MARE ISLAND NAVAL SHIPYARD		5 TYPE OF REPORT & PERIOD COVERED Final; Oct 81 – Sep 82 6 PERFORMING ORG. REPORT NUMBER
7 AUTHOR(s) J. A. Bailard and J. M. Camperman		8 CONTRACT OR GRANT NUMBER(s)
9 PERFORMING ORGANIZATION NAME AND ADDRESS NAVAL CIVIL ENGINEERING LABORATORY Port Hueneme, California 93043		10 PROGRAM ELEMENT PROJECT TASK AREA & WORK UNIT NUMBERS 63725N; YO995-01-002-999
11 CONTROLLING OFFICE NAME AND ADDRESS Naval Facilities Engineering Command Alexandria, Virginia 22332		12 REPORT DATE May 1983 13 NUMBER OF PAGES 64
14 MONITORING AGENCY NAME & ADDRESS(if different from Controlling Office)		15 SECURITY CLASS (of this report) Unclassified 15a DECLASSIFICATION DOWNGRADING SCHEDULE

16 DISTRIBUTION STATEMENT (of this Report)

Approved for public release; distribution unlimited.

17 DISTRIBUTION STATEMENT (of the abstract entered in Block 20, if different from Report)

18 SUPPLEMENTARY NOTES

19 KEY WORDS (Continue on reverse side if necessary and identify by block number)

Dredging, reduction, scour, jets, turbulent, sedimentation, control

20 ABSTRACT (Continue on reverse side if necessary and identify by block number)

In response to rising dredging costs, the Navy has developed a number of concepts for sedimentation control systems, which serve as alternatives to conventional dredging. One concept, the scour jet array, prevents sedimentation through the scouring action of submerged near-bottom water jets. This report presents the design of a scour jet array test bed which will be used to verify proposed scour equations and to evaluate new design technology. The

continued

DD FORM 1 JAN 73 1473 EDITION OF 1 NOV 65 IS OBSOLETE

Unclassified

SECURITY CLASSIFICATION OF THIS PAGE (When Data Entered)

20. Continued

66-jet array covers a total of 366 m (1,200 ft) of quay wall and is capable of scouring to distances of 30 m (98 ft) from the wall. The jet array is powered by a 0.379 m^3/sec (6,000 gpm), 336 kW (450 hp) vertical turbine pump. An automatic control system is included that utilizes pneumatically actuated valves and a microprocessor controller. The microprocessor also serves as an instrumentation data logger, facilitating testing as well as routine operational checking.

Library Card

Naval Civil Engineering Laboratory
A DESIGN FOR A TEST BED SCOUR JET ARRAY FOR MARE ISLAND NAVAL SHIPYARD (Final), by J. A. Bailard and J. M. Camperman
TR-899 64 pp illus May 1983 Unclassified

1. Dredging 2. Sedimentation I. YO995-01-002-999

In response to rising dredging costs, the Navy has developed a number of concepts for sedimentation control systems, which serve as alternatives to conventional dredging. One concept, the scour jet array, prevents sedimentation through the scouring action of submerged near-bottom water jets. This report presents the design of a scour jet array test bed which will be used to verify proposed scour equations and to evaluate new design technology. The 66-jet array covers a total of 366 m (1,200 ft) of quay wall and is capable of scouring to distances of 30 m (98 ft) from the wall. The jet array is powered by a 0.379 m^3/sec (6,000 gpm), 336 kW (450 hp) vertical turbine pump. An automatic control system is included that utilizes pneumatically actuated valves and a microprocessor controller. The microprocessor also serves as an instrumentation data logger, facilitating testing as well as routine operational checking.

CONTENTS

INTRODUCTION

Navy harbors have historically been located in estuaries, which provide natural quiet water berthing areas. Over the years, these harbors have been deepened in response to an increase in the draft of Navy vessels. This deepening, however, has upset the natural equilibrium of the estuaries leading to increased sedimentation and the need for continual maintenance dredging.

Sedimentation in estuaries results principally from the flocculation of clay particles. These particles are transported by rivers to the estuary in a largely dispersed state. Upon coming in contact with the more saline estuarine water, flocculation occurs, causing the particles to aggregate and settle to the bottom. There they form a concentrated fluid mudlike layer, which is transported by currents to quiet water areas. When it comes to rest on the bottom, the fluid mud layer quickly consolidates, increasing in strength and becoming part of the bottom sediments.

Rates of sedimentation in Navy harbors vary with location as well as with season. Highest rates of sedimentation are found at Mare Island Naval Shipyard, Charleston, and Alameda, where they can be as great as 3 meters (10 feet) per year (Malloy, 1981). Greatest rates generally occur between January and June, due to the increased river-borne sediment flux into the estuary. Field studies (Jenkins et al., 1981), however, suggest that the sedimentation can often be episodic, occurring during brief periods when the sediment abundance is high and the water salinities exceed approximately 7 ppt. Since the sediment abundance increases with increasing river discharge while the salinity decreases, optimum conditions for sedimentation reflect a delicate balance between these two variables.

The above processes present the Naval Facilities Engineering Command (NAVFAC) with the never-ending need to perform maintenance dredging in most Navy harbors. Rising energy costs coupled with more stringent environmental constraints on dredge material disposal have caused the annual cost of dredging to substantially increase in recent years. Currently, the Navy's annual maintenance dredging cost is estimated to be $23 million (Malloy, 1980). This cost is projected to increase due to increase dredging volumes associated with increasing ship drafts. Clearly, alternatives to conventional dredging are needed. Responding to this need, NAVFAC funded the Naval Civil Engineering Laboratory (NCEL) to initiate a research program to develop innovative alternatives to dredging. This program, performed largely by contract to Scripps Institution of Oceanography, resulted in the development of several different experimental systems, among which is the scour jet array.

Referring to Figure 1, a typical scour jet array consists of a series of submerged water jets which sweep newly deposited mud out of a berthing area. The jets are sequentially activated on an ebbing tide so that the scoured sediment is carried from the general area.

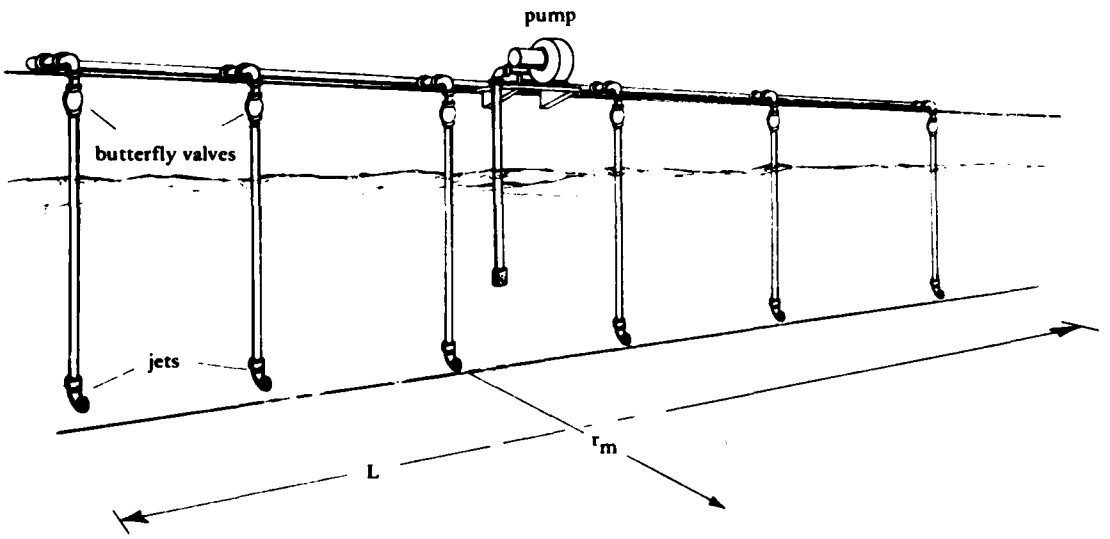

Figure 1. Conceptual sketch of a scour jet array with a length L and a scour radius r_m.

Following its conception, laboratory and field research was conducted to determine the performance of a scour jet array. The laboratory research (Van Dorn et al., 1975, 1977; Jenkins et al., 1981) sought to develop relationships between the effective scour radius of a jet and its flow rate, diameter, angle and height. The field research (Van Dorn et al., 1978; Jenkins et al., 1981) served to partially verify these relationships; a more important function was to validate the overall concept of using a jet array as an alternative to dredging. Details of the laboratory and field tests are discussed in a later section of this report.

Although the above field tests served to validate the operational feasibility of a scour jet array, several important questions remained to be answered before the design of an array could be viewed as being routine. These questions included:

1. Can the laboratory-derived shear stress equations be directly applied to prototype scour jet arrays?

2. What is the optimum shear stress for scouring newly deposited fluid mud as well as more fully consolidated mud deposits?

3. How can a scour jet array be made more compatible with waterfront operations?

4. What are the best materials and components to use in a scour jet array?

To answer these questions, a test bed array was proposed. The array is to be installed at Mare Island Naval Shipyard (MINSY) along a quay wall fronting Mare Island Strait (Figure 2). Discussions with MINSY personnel suggested that a 366-meter- (1,200-foot-) long array capable of scouring to distances of 20 to 30 meters (66 to 98 feet) would be most suitable. This report contains a discussion of the design of the test bed array, its components, and a plan for conducting tests designed to answer the above-stated questions.

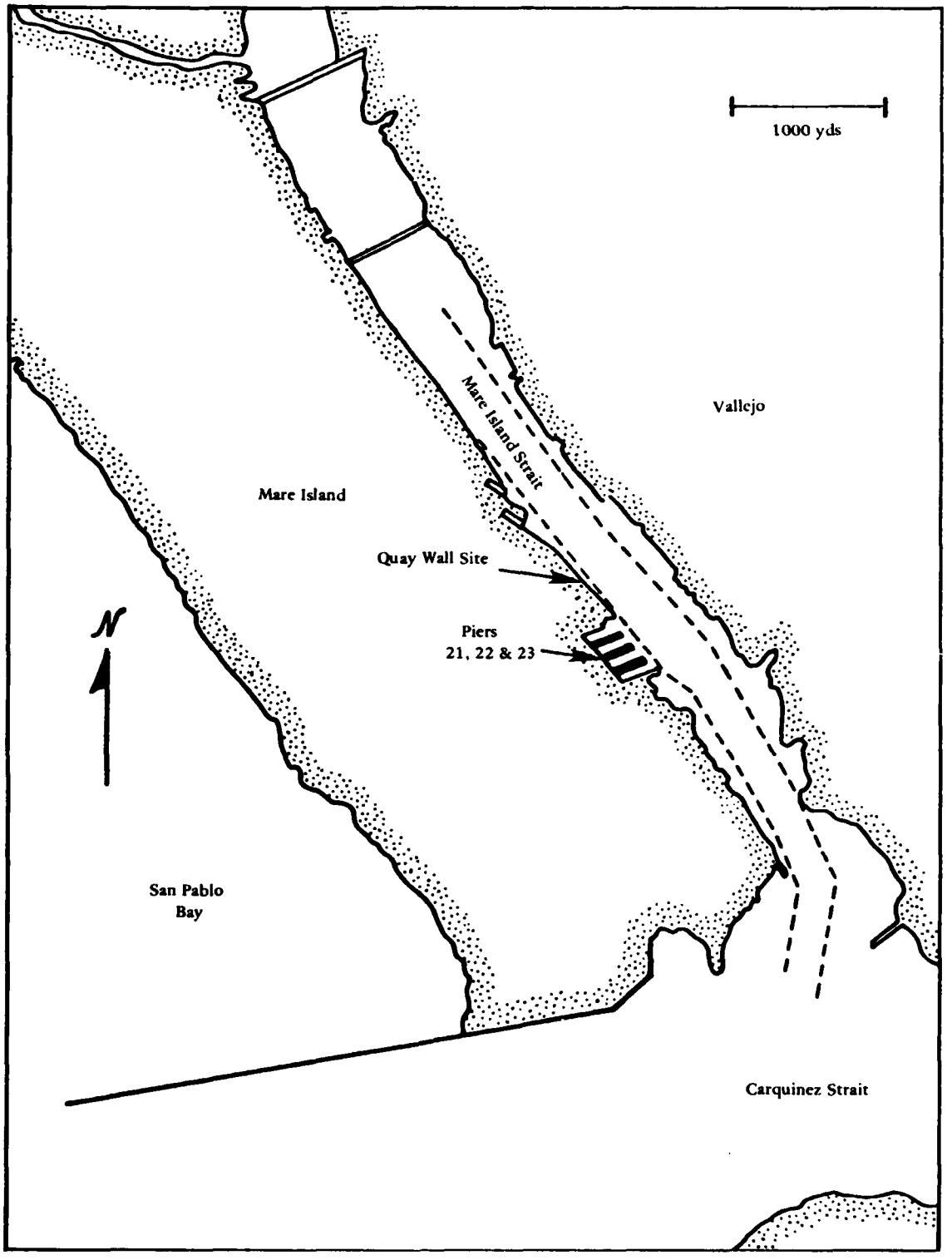

Figure 2. Location map of Mare Island Naval Shipyard and vicinity, San Francisco, California.

OBJECTIVE

The overall objective of the study was to design a scour jet array capable of systematically verifying two laboratory-based jet scour equations. Secondary objectives were to evaluate the performance of a number of components and materials that have not been used in previous arrays, and to make the system more compatible with waterfront operations. A final objective was to design an array that would be suitable for long-term use following the end of the testing program.

It is noteworthy that because the array will be used as a test bed, it was designed to be considerably over-powered in order to provide added flexibility in testing. As a result, it should not be viewed as being typical of future operational scour jet arrays in all respects. In fact, a more conventional array meeting a need for scouring to 20 meters (66 feet) and having fixed rather than variable jet characteristics is estimated to cost approximately half as much and use one-fourth the power.

Following a review of shipyard requirements and of scour jet array limitations, the following test bed performance objectives were identified:

1. Variable scour distances from 10 to 30 meters (33 to 98 feet)

2. Variable jet duty cycle time from 1.5 to 48 minutes

3. Variable jet angle between 0 and 30 degrees

4. Variable jet height between 0 and 4 meters (0 to 13 feet) off the bottom

5. Total cycle time for the array less than 6 hours

PREVIOUS TEST RESULTS

The concept of a scour jet array was first proposed by Van Dorn et al. (1975). Subsequent laboratory tests were made at Scripps Institution of Oceanography with the objective of predicting the range of scour in front of a horizontal, near-bottom jet as a function of the jet diameter and the discharge velocity. After extensive experiments using a thin layer of diatomaceous earth as a scour indicator (movement occurs at a stress of about 0.1 Pa (1.45×10^{-5} psi)), Van Dorn et al. (1977, 1978) and Jenkins et al. (1981) produced the following equation for the maximum jet scour radius, r_m, in front of a horizontal, near-bottom jet

$$\left(\frac{r_m}{d}\right)^{2.4} = \frac{120\ \rho\ u_o 2}{\tau\ R_e^{0.4}} \qquad (1)$$

where τ = the shear stress sufficient to initiate scour (typically 0.4 Pa (5.8×10^{-5} psi))

u_o = jet discharge velocity

d = jet diameter

ρ = fluid density

R_e = jet Reynolds number, $(u_o d/\nu)$

ν = kinematic viscosity of the fluid

For a horizontal, near-bottom jet, the scour pattern is tear-drop shaped with the maximum width, y_m, equal to $r_m/3$ and occurring at a distance of 0.67 r_m from the jet (Figure 3). Recent tests at NCEL (see Appendix A) have shown that the scour pattern is also a function of the height of the jet from the bottom, h, and its angle relative to the horizontal, θ. For a raised and angled jet, the maximum distance of scour is described by

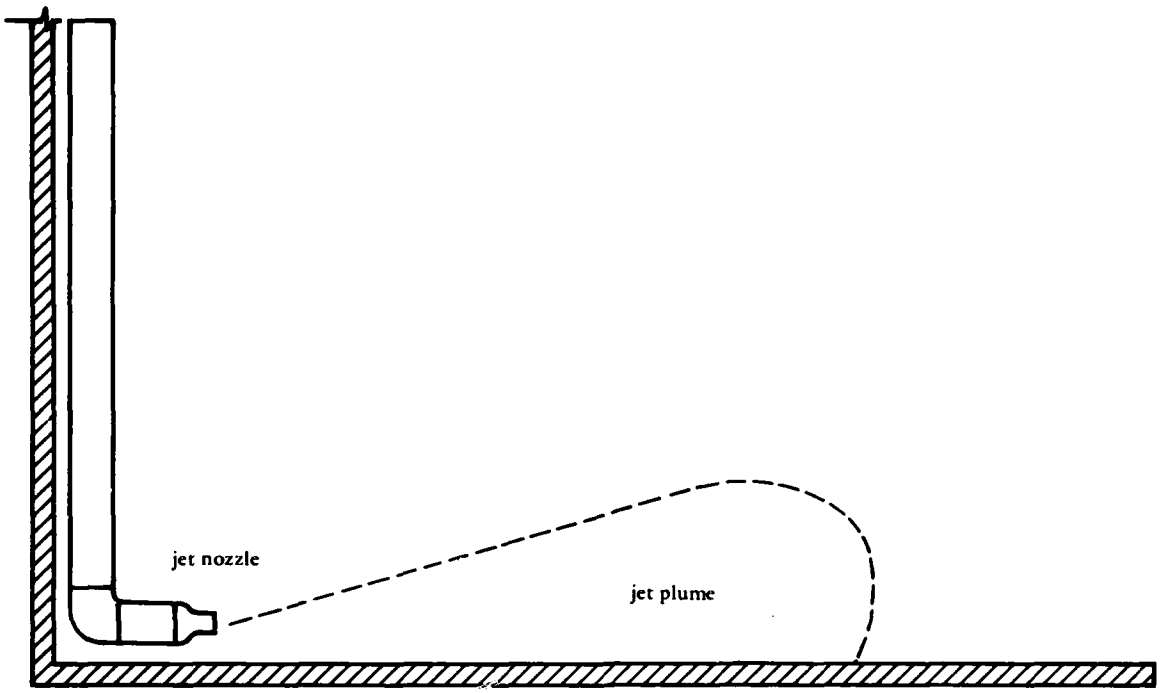

side view

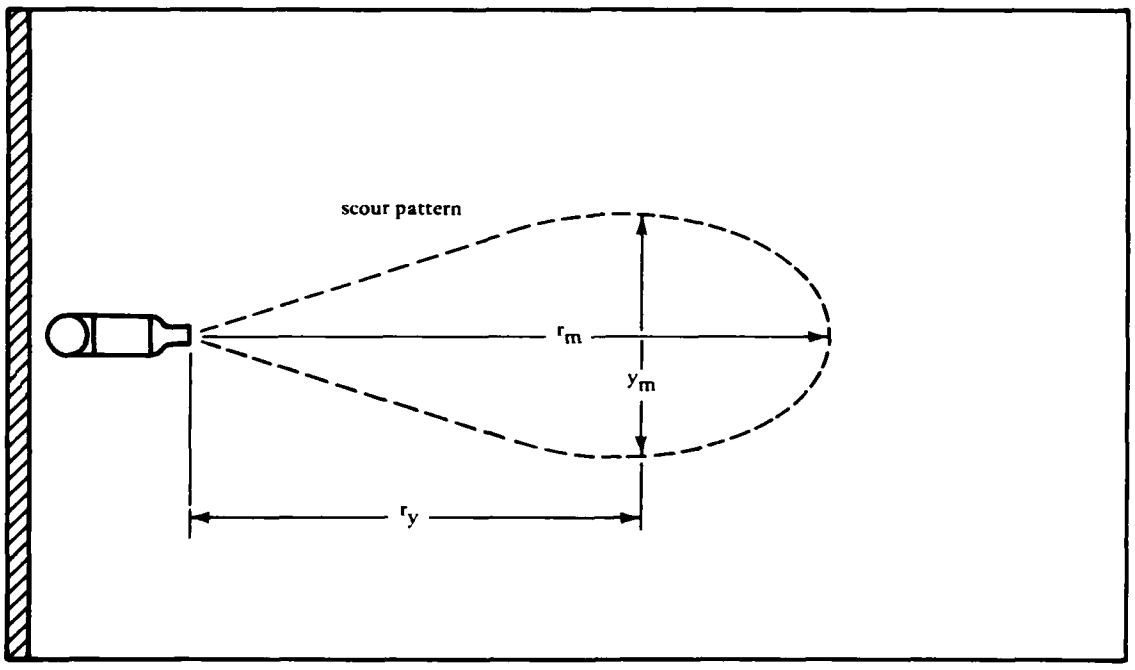

top view

Figure 3. Definition schematic for horizontal bottom-mounted jet.

$$\frac{r_m}{d} = \left(\frac{\tau \, R_e^{0.4} \times 10^4}{C_o \, \rho \, u_o^2} \right)^{C_1} \tag{2}$$

where

$$C_o = 10^{(-C_2/C_1)} \tag{3}$$

$$C_1 = 0.0533 \sin (5.59\,\theta) - 0.385 + (-0.0201 + 0.00593\,\theta^{0.356}) \frac{h}{d} \tag{4}$$

$$C_2 = 2.442 + 0.0108 \frac{h}{d} - 1.266 \times 10^{-4} \left(\frac{h}{d}\right)^2 - 0.0118\,\theta - 9.33 \times 10^{-5}\,\theta^2 \tag{5}$$

where h = height above the bottom

θ = downward angle of the jet relative to horizontal

Equation 2 was developed from data having a range in variables $0 \leqq \theta \leqq 30°$ and $1.3 \leqq h/d \leqq 45.4$. Its validity outside these bounds is untested. Note that for $\theta = 0$ and $h/d \sim 1.0$, Equation 2 becomes essentially equal to Equation 1.

In addition to affecting the maximum scour distance, r_m, the variables h and θ were also found to affect the shape of the scour pattern. As h and θ are increased, the shape becomes more rounded. Increasing h alone causes the pattern to shift away from the jet. Referring to Figure 4, a new variable, s, was introduced to describe the horizontal distance from the jet to the initiation of scour. Despite considerable effort, analytic expressions such as Equations 1 and 2 could not be found for predicting the width of the pattern, y_m, the radius of maximum width, r_y, nor the distance to initial scour, s. Instead, graphical solutions are offered in Appendix A.

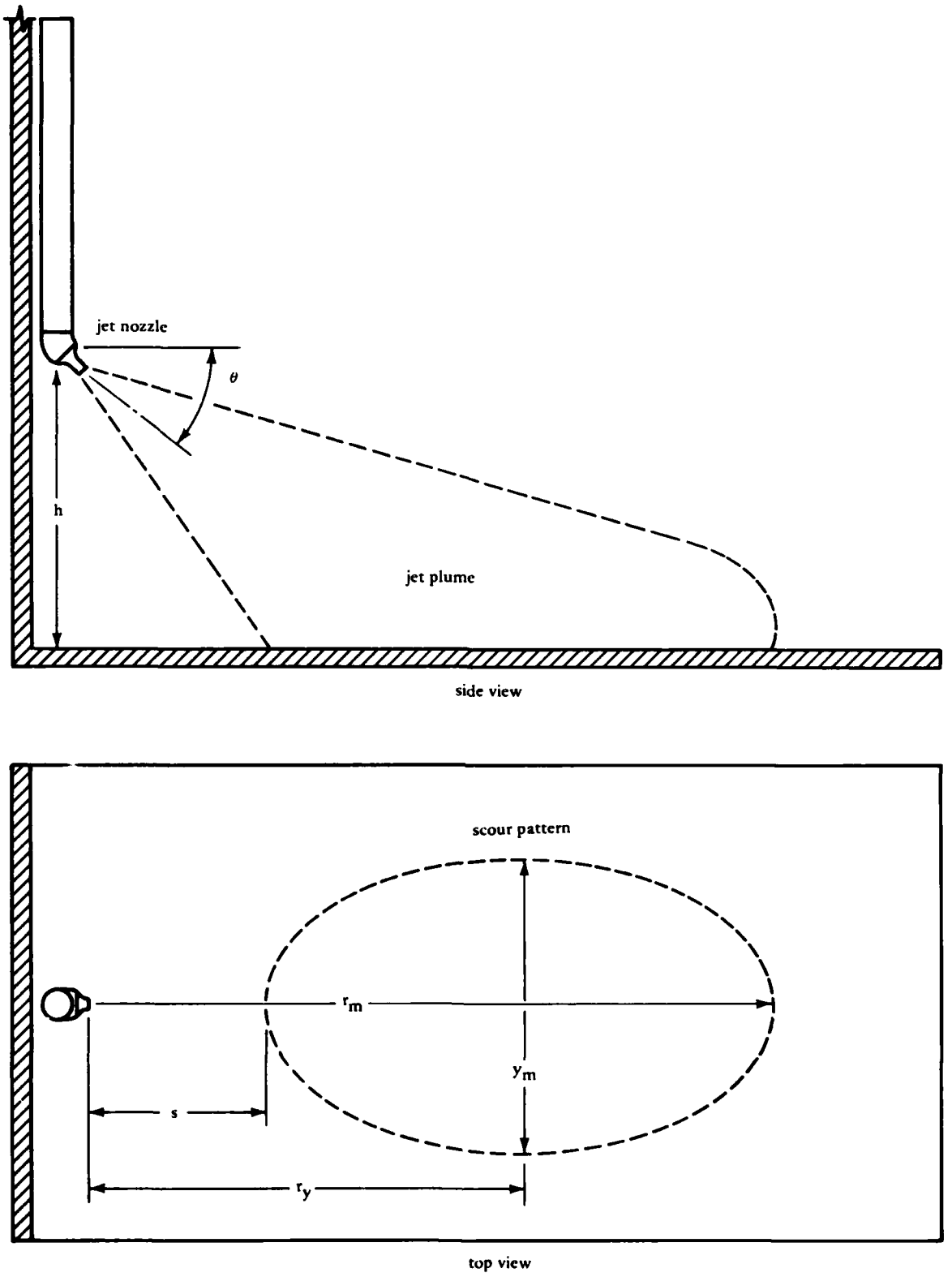

Figure 4. Definition schematic for angled, elevated jet.

One of the uncertainties in using Equations 1 and 2 to predict the scour radius of a jet is deciding what shear stress, τ, is necessary to scour cohesive sediment. A number of early laboratory studies addressed different aspects of this question, including those by Partheniades (1965), Ariathurai and Arulanandan (1972), Arulanandan (1975), and Van Dorn et al. (1975). In general, these studies suggested that the critical stress for sediment erosion is about 0.1 Pa (1.45×10^{-5} psi) but that it varies with the physiochemical properties of the soil and the interstitial water. In all cases, higher shear stresses cause an exponential increase in the rate of scour.

More recently, the relative effects of salinity, water content, and temperature of the mud on the rate of scour were systematically studied by Gularte (1978). He found that the rate of scour for a given shear stress increased with decreasing salinity, increasing temperature, and increasing water content. The latter parameter is particularly important because Va Dorn et al. (1975) found that the water content of the fluid mud decreases hyperbolically with time, the mud typically experiencing a 50% compaction during the first 24 hours after deposition. For salinities on the order of 10 ppt, Gularte found that this compaction would increase the critical shear stress from approximately 0.1 Pa to 0.2 Pa (1.45×10^{-5} to 2.90×10^{-5} psi). Ultimate compaction would produce a threshold stress in excess of 0.4 Pa (5.8×10^{-5} psi).

In addition to the above laboratory tests, three different prototype jet arrays have been designed, installed, and tested by Scripps Institution of Oceanography (Van Dorn et al., 1978; Jenkins et al., 1981). The first jet array was an area type of array in which 70 jets were used to protect a 20 x 30-meter (66 x 98-foot) area of bottom (Figure 5). The jets were operated in groups of 10 and were powered by a 112-kW (150-hp) centrifugal pump. With a total flow rate of 0.110 m^3/sec (1,600 gpm) and a pressure of 690 kPa (100 psi), the 0.02-meter-(0.066-foot-) diam jets were capable of producing a shear stress in excess of 0.5 Pa (7.25×10^{-5} psi) throughout the entire 20 x 30-meter (66 x 98-foot) area.

The jet array was operated on a daily basis during the period of ebb tidal flow. Each group of jets was operated for a period of 7 minutes, producing a total system cycle time of 49 minutes per tidal cycle.

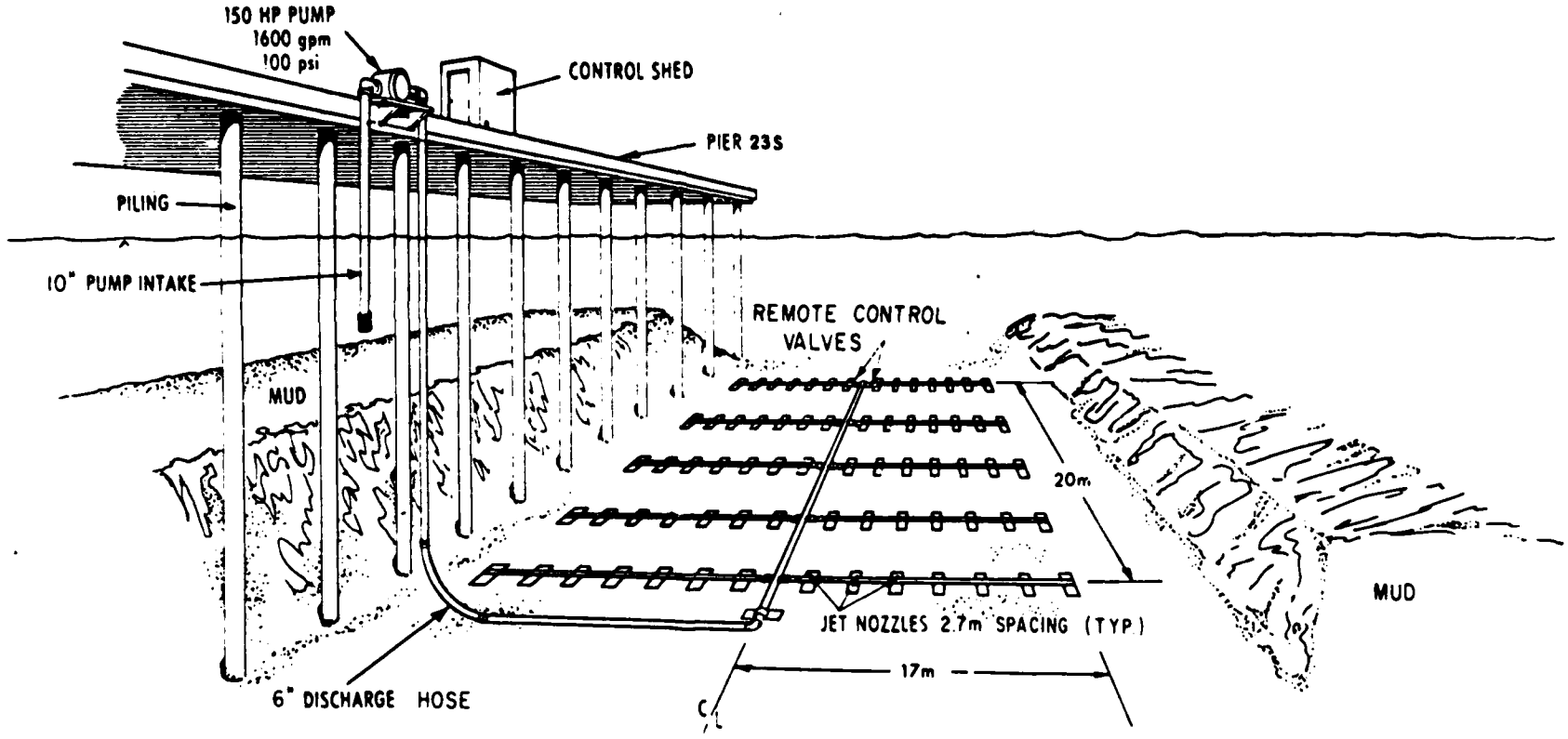

Figure 5. Prototype 70-jet array installed 17 Feb 77 at Mare Island Naval Shipyard.

During the 4-month period when this system was operated, the jet array performed as designed, preventing any sedimentation from occurring in the protected area. At the same time, sedimentation within an adjacent control area totaled 0.75 meter (2.5 feet). After 3 months, the array began to experience problems with the control valves. These valves were a type of pneumatic actuated pinch valve utilizing a collapsible inner liner. The valves were closed by pressurizing the cavity between the outer body of the valve and an inner rubber liner. The air pressure causes the liner to squeeze shut, pinching off the flow. Valve failure occurred when the liner became perforated. After a period of 4 months, the supply of spare valve liners (2) had been depleted. At this point the experiment was terminated since it had become clear that valve failure would be a continual problem.

The second scour jet array to be field tested was a linear type of array similar to that shown in Figure 1. The array was 65 meters (212 feet) long and was mounted to the side of a quay wall adjacent to a submarine berth. The array consisted of 25 jets operated in groups of 5 jets. The array was powered by the same pump and motor used in the first array. The control valves were also the same, however, the jet duty cycle was extended to 12 minutes. The jets were 0.03 meter (0.098 foot) in diameter and the flow rate through each jet was 0.024 m^3/sec (379 gpm). If the jets had been bottom-mounted and horizontal, they would have been expected to produce a stress of 0.1 Pa (1.45×10^{-5} psi) at a distance of 17 meters (56 feet) or, alternatively, a stress of 0.5 Pa (7.25×10^{-5} psi) at a distance of 9 meters (30 feet). As installed, however, the jets were mounted on the wall at a point 4.3 meters (14 feet) above the freshly dredged bed and angled downward 25 degrees from the horizontal. The reason for elevating the jets was to avoid eroding a rip-rap rock toe at the base of the wall.

The elevation of the jets and the contouring effect of the toe make it difficult to estimate the shear stress distribution. Presumably the stress at 9 meters (30 feet) was less than 0.5 Pa (7.25×10^{-5} psi), but just how much less is open to question. Equation 2 cannot be applied with confidence because h/d is greater than 45 and the effect of the toe is unknown.

The jet array was operated for a period of 5 months during which time three pinch valve failures occurred. After 50 days of operation, the fathometer surveys showed that the effective scour distance was about 6 meters (20 feet). Increasing the jet duty cycle from 12 minutes/jet to 48 minutes/jet increased the scour radius to about 8 meters (26 feet). Some scouring action was evident as far away as 30 meters (102 feet), but the effectiveness of the scouring action decreased almost linearly with distance. For example, at a distance of 15 meters (49 feet), 65% of the shoaling that occurred in an adjacent control area was prevented by the array.

These results tend to support the findings of Gularte (1978). Apparently at distances in excess of 6 meters (20 feet), the volume of mud eroded in a 12-minute period of time was less than the volume of mud deposited. Increasing the jet duty cycle increased the scour radius to some degree, but not substantially, since the rate of erosion falls off exponentially with distance. This would suggest that short periods of high stress are more effective at scouring than longer periods of low stress.

Because of the limited scour radius of the second array, a third linear array was designed and tested. This array was also attached to the face of a quay wall, and covered a distance of 63 meters (206 feet) along the berth. Each of the 10 jets were 0.073 meter (0.239 foot) in diameter and were individually operated in a sequential manner. Again, the same pump was used except that the diameter of the pump impeller was reduced to produce a flow rate of 0.121 m^3/sec (1,910 gpm) with a pressure of 634 kPa (92 psi). The duty cycle time for each jet was 12 minutes.

Similar to the previous array, the jets were located 4.6 meters (14 feet) above the bottom and were oriented downward at an angle of 25 degrees. If the jets had been bottom-mounted and horizontal, they would have produced a shear stress of 0.4 Pa (5.8×10^{-5} psi) at a distance of 20 meters (66 feet). Because of their altered geometry, however, this distance would be expected to be less. Based on Equation 2, a stress of 0.4 Pa (5.8×10^{-5} psi) would be expected at a distance of 10.6 meters (35 feet). The presence of the sloping toe at the

base of the quay wall, however, is expected to extend the scour distance to a value closer to 20 meters (66 feet); however, the exact distance of the 0.4-Pa (5.8×10^{-5}-psi) shear stress contour is unknown.

This third array was operated during ebb tide on a daily basis for a period of about 2 years. During this time, numerous interruptions and failures occurred, mostly due to power interruptions, mounting system failures, and pinch valve failures. In spite of these difficulties, the array was found to prevent daily sedimentation out to a distance of approximately 21 meters (69 feet). In addition, it was found that after a period of inactivity, the array was able to excavate consolidated mud out to a distance of 15 meters (49 feet).

The experience of the three field tests can be summarized as follows:

1. A scour jet array is a successful concept for minimizing dredging in difficult access areas.

2. A shear stress of 0.4 to 0.5 Pa (5.8×10^{-5} to 7.25×10^{-5} psi) appears to be adequate for scouring newly deposited mud from berthing areas. Lower stresses are probably adequate as well, but the presence of the mud and rock toe at the base of the quay wall at the test site makes an accurate determination from these tests impossible at this time.

3. Short periods of high shear stress levels appear to be superior to longer periods of lower stress levels for removing newly deposited mud. (Most of the evidence for this is based on laboratory experiments.)

4. The pneumatic pinch valves tested were inappropriate for use at the pressures and flow rates encountered in the first three arrays.

5. Scour jet array systems must be robust and fail-safe to perform successfully in a waterfront environment.

Questions which remain unanswered are as follows:

1. Do Equations 1 and 2 adequately describe the shear stress distribution under prototype conditions?

2. What is the optimum stress level for use in designing a scour jet array?

3. What types of materials and components are best to use in a permanent scour jet array?

These questions and others will be addressed by the proposed test bed scour jet array.

SYSTEM DESIGN APPROACH

The test bed scour jet array is shown schematically in Figure 6. Appendix B contains detailed engineering drawings. The following discussion illustrates the approach that was used in the design of the scour jet array.

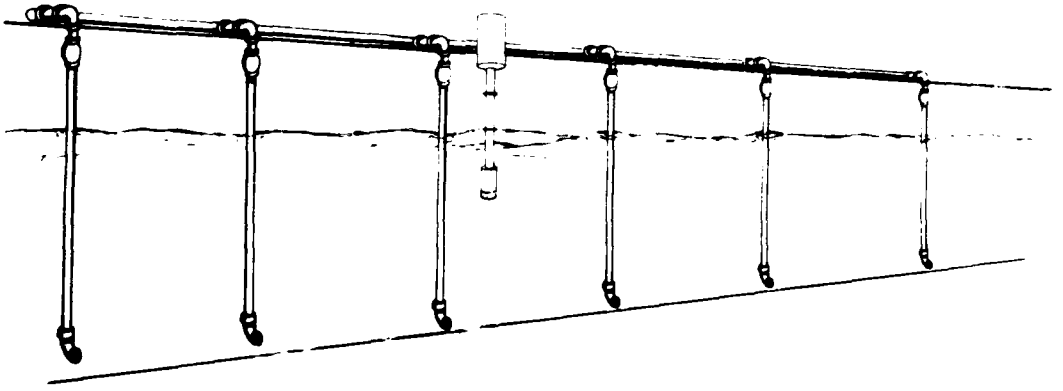

Figure 6. Conceptual representation of test bed scour jet array.

Objectives and Constraints

One of the challenges of designing the test bed scour jet array was to satisfy a wide range of constraints on the system. The basic design constraints were as follows:

1. The array is to be 365 meters (1,200 feet) long and capable of scouring to distances of at least 20 meters (66 feet). In this way the array can protect two complete submarine berths and will be useful to MINSY over the full lifetime of the system (estimated to be approximately 10 years).

2. The array must not interfere with shipyard activities in the quay wall area. This area is heavily congested with men and equipment engaged in overhauling submarines.

3. The array must be as robust as possible so as to minimize the potential for damage. Components must be generally replaceable without the need for divers.

4. The array must be remotely operated and controlled. MINSY personnel will not be available for continual monitoring of the array's operation.

Within the above constraints the jet array design was open to variation. The previously defined test objectives, however, served to fix the remainder of the basic design. These objectives were as follows:

1. Variable scour distances from 10 to 30 meters (33 to 98 feet).

2. Variable jet duty cycle time from 1.5 to 48 minutes.

3. Variable jet angle from 0 to 30 degrees.

4. Variable jet height from 0 to 4 meters (0 to 13 feet).

5. Total system cycle time less than 6 hours.

Geometry and Flow Conditions

The design approach used to specify the geometry and flow conditions for the array was as follows:

1. The nominal scour radius, r_m, was defined as 20 meters (66 feet). Past experiments (Van Dorn et al., 1977) had shown that a 10% overlap in scour patterns resulted when the jet spacing is $r_m/3.3$. Based on this criterion, a jet spacing of 6.1 meters (20 feet) was initially selected. With a 365-meter (1,200-foot) array, this spacing

resulted in a total of 61 jets. Later discussions with MINSY personnel revealed that the quay wall fender piles were spaced 1.83 meters (6 feet) apart. As a result, the jet spacing was made to be the nearest even multiple of 1.83 meters, or 5.45 meters (18 feet).

2. The maximum desired scour distance was approximately 30 meters (98 feet). Based on previous field tests of scour jet arrays (Jenkins et al., 1981), a 0.5-Pa (7.25×10^{-5}-psi) shear stress was used to define the scour distance. Close examination of Equations 1 and 2 reveals that fixing the scour radius, r_m, and the required stress, τ, does not uniquely determine the jet diameter, d, nor the jet discharge velocity, u_o. In general there is a trade-off between systems with high flow rates, low heads, and low energy consumption versus systems with low flow rates, high heads, and high energy consumption. Presented with this choice, one approach (Bailard, 1980) is to select a system with the lowest annual cost. In the present case, however, this produces a system having piping too large to be easily fit onto the quay wall face. In the present case, the diameter of the pipe manifold was selected to be as large as possible while still allowing adequate clearance for fittings and installation. The resulting pipe sizes were 0.304 meter (1 foot) for the manifold pipe and 0.254 meter (0.833 foot) for the vertical riser pipes.

3. Having selected the above pipe sizes, the pump and jet nozzle sizes were determined from the scour jet Equation 1 coupled with the usual pipe head loss equations (see Appendix C). As discussed in the test plans, four flow conditions were used in the array. These conditions correspond to nominal scour distances of 10, 15, 20, and 30 meters (33, 49, 66, and 98 feet). As a means of keeping the pump operating point constant, it was decided to keep the jet discharge pressure constant for all of the jets and to vary the jet flow rate by changing the number of jets in a group to be operated at once. The total flow would remain constant. For design purposes a worst case was assumed where the scour distance of 30 meters (98 feet) was desired for the jet farthest from the pump. Using the equations developed in Appendix C, a jet

diameter of 0.147 meter (0.482 foot) was found to be optimum, requiring a pump with a flow rate of 0.416 m^3/sec (6,580 gpm) and a head of 62 meters (202 feet). Assuming a nominal pump efficiency of 0.85, the required motor size would be approximately 295 kW (395 hp).

4. The above conditions were theoretical optimums. In selecting a pump, it was found to be necessary to alter the operating conditions slightly to fit actual pump curves. The selected pump, thus, has a flow rate of 0.379 m^3/sec (6,000 gpm), a head of 65.8 meters (216 feet), and an efficiency of 0.85. The required horsepower for the pump is 295 kW (395 hp); however, a 336-kW (450-hp) motor was selected to provide a margin of reserve power. Under these operating conditions, the required jet diameter was 0.131 meter (0.43 foot), resulting in an estimated scour distance of 30 meters (98 feet).

5. For nominal scour distances of 10, 15, and 20 meters (33, 49 and 66 feet), the pump flow rate will be split between 15, 6, and 3 jets, respectively. In order to keep the pump operating point constant, the jet diameters required for these conditions are 0.0338 meter (0.111 foot), 0.0537 meter (0.176 foot), and 0.0759 meter (0.249 foot), respectively. Using Equation 1, the predicted scour distances are estimated to be 9.6 meters (31.5 feet), 14.0 meters (46.1 feet), and 18.8 meters (61.6 feet), respectively.

6. For jets located at intermediate distances from the pump, the head losses in the piping will be less, and an additional head loss will be needed to maintain the same operating point for the pump. This added loss will be obtained by limiting the degree of opening of the pneumatic actuated control valves via adjustable limit stops. This feature will permit careful fine tuning of the array after construction to ensure uniform operating conditions for all jets. Such conditions are necessary in order to systematically examine the validity of Equations 1 and 2.

The above design calculations assumed a required shear stress of 0.5 Pa (7.25×10^{-5} psi). The actual stress required to scour the mud may vary somewhat. Additionally, the design calculations were based on Equation 1, which is valid for horizontal, bottom-mounted jets. The actual installation of the jets (see Appendix B) requires that even the lowest jets be elevated 2.59 meters (8 feet) above the dredging project depth. The angle of these jets will be 5 degrees. Because Equation 2 remains largely untested, however, it was not used in the design calculations. One of the objectives of the test bed jet array will be to resolve these uncertainties.

Control System and Instrumentation

While the basic objective of the test bed scour jet array was to systematically test the validity of the scour Equations 1 and 2, it was also considered desirable to have a system which was as flexible as possible. For this reason, a microprocessor was chosen both to control the system and to serve as a data logging device. Previous experience with a mechanical cam-type controller (Van Dorn et al., 1978; Jenkins et al., 1981) had shown the need for greater ease of modification. Similar dockside experience with other automatic control devices suggested that the use of pneumatic control valves was desirable.

COMPONENT DESCRIPTION

The jet array, as shown in Figure 6, consists of the pump, piping, valves, the controller, and the instrumentation system. The following is a description of each major component. Additional details may be found in Appendixes B and D.

Pump

Jet array pumping requirements called for a flow rate of 0.379 m^3/sec (6,000 gpm) and a head of 65.8 meters (216 feet). Following discussions with MINSY personnel, it was decided that a vertical

turbine pump would be least disruptive to quay wall activities due to its compact configuration (Figure 7). This type of pump also has the added advantage of a submerged impeller, eliminating the need for elaborate priming mechanisms. For the present system, a Layne Bowler Inc. vertical turbine pump, model 19GH, was selected. The pump has a 6-meter- (20-foot-) long, 35.6-cm- (1.17-foot-) diam column and a fabricated head. Power to the pump is provided by a 336-kW (450-hp), 480-volt motor rotating at 1,760 rpm. At the base of the pump is an intake strainer. The bowl assembly is cast iron with bronze fittings. The column and head assemblies are ASTM AS3 steel while the shaft is stainless steel with a diameter of 0.049 meter (0.162 foot). The entire pump, column, and head assembly is coated with a fusion-bonded epoxy.

The pump is supported by a steel platform attached to the side of the quay wall. The steel platform will be galvanized for corrosion protection. Design of the platform is such that the pump and motor assembly does not project more than 0.60 meter (2 feet) beyond the outer edge of the quay wall timber fendering system. Protection for the pump and motor assembly will be provided by additional wooden pilings and timbering positioned on each side of the pump.

Pipe

The scour jet array piping consists of two elements: the manifold pipe, 0.3 meter (1 foot) in diameter; and the vertical riser pipes, 0.25 meter (0.833 foot) in diameter. Both sizes of pipe will be fiberglass, schedule 40. Other types of pipe including polyvinylchloride and coated steel were considered but were discarded because of their fragility (PVC) and their potential for corrosion (steel).

Pipe fittings and connectors for the pipe will primarily be the Kwikey® type, manufactured by Fiberglass Resources Inc. (Figure 8). This type of connector facilitates installation and minimizes repair time if components need replacement. In addition, this type of connection is corrosion proof. Flange connectors will be used at the control valves.

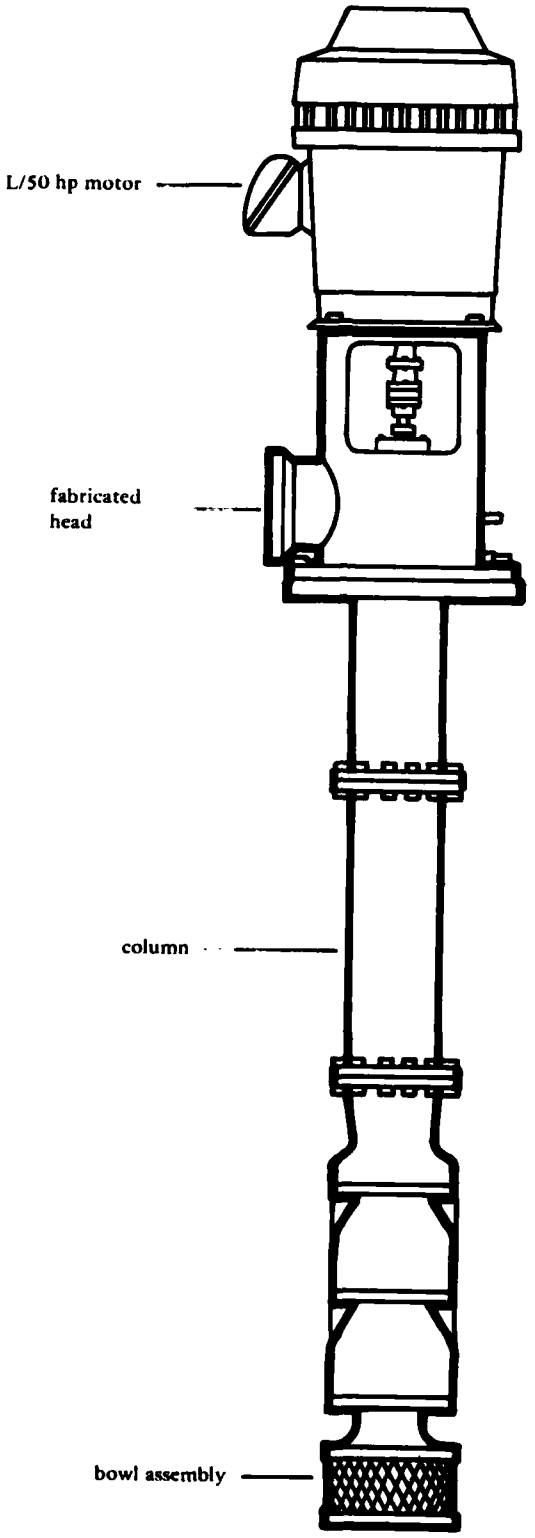

Figure 7. Schematic view of vertical turbine pump.

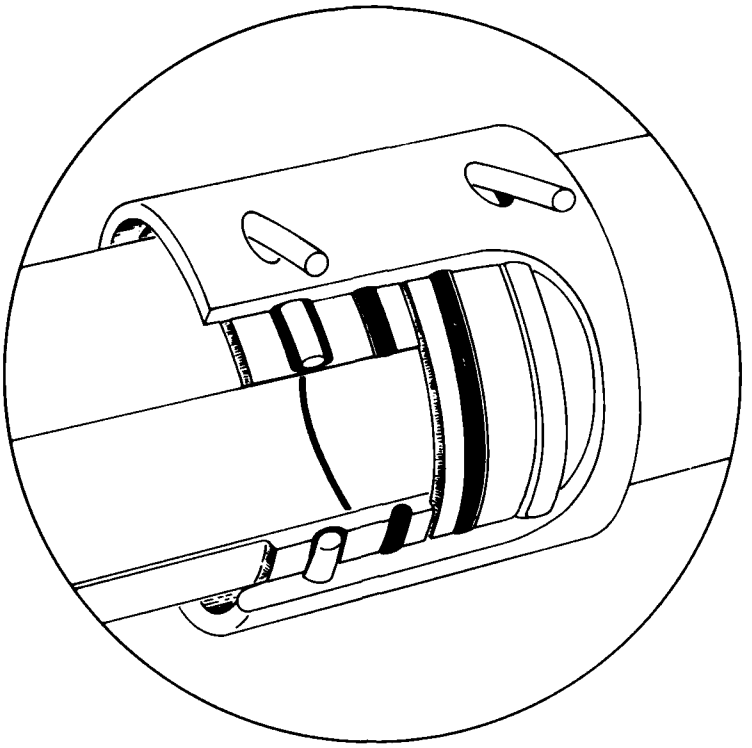

Figure 8. Schematic diagram of pipe connectors.

Valves

Due to problems with corrosion and exposure, MINSY personnel have found pneumatic control systems to be most satisfactory for dockside service. This is especially true in the present case where the automatic control valves will be submerged in water by as much as a foot from time to time. In the previous three scour jet array systems, pneumatic pinch valves were used for service underwater. These were found to be a constant source of problems due to failure of the liners after approximately 4 months. Further compounding the problem were difficulties in scheduling divers to repair the valves.

As a result of the above problems, pneumatically actuated butterfly valves were selected for the present system (Figure 9). The valves are located just below the manifold pipe to make servicing as simple as possible. The selected valves are 0.25 meter (0.833 foot) in diameter, manufactured by Keystone International Inc., Model 139-943. The valves have a nickel aluminum body with an aluminum-bronze disc and a monel shaft.

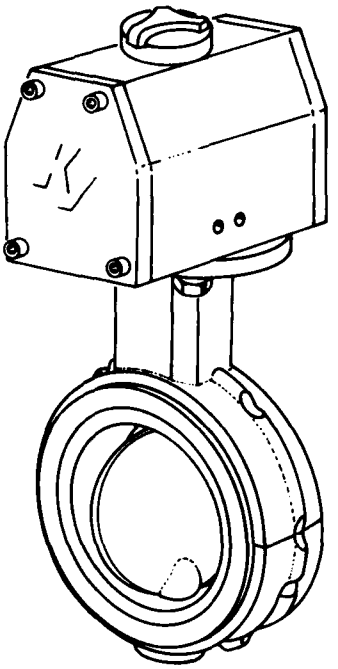

Figure 9. Schematic diagram of pneumatic actuated butterfly valves.

The actuator is a double-acting pneumatic rotary actuator manufactured by Keystone International, Model F79-500. These actuators have a rack-and-pinion type of action making them very compact and completely submersible. The housing of the actuator is zinc-coated cast iron with stainless steel fasteners. The above materials represent a compromise to give the desired 10-year longevity at a reasonable cost.

Control and Instrumentation System

The primary purpose of the control system is to activate the jet array just after the start of ebb tide and then to sequence the jets through a preset pattern of duty cycles. In addition, the control system must act as a monitor and data logger to ensure proper operation of the jet array. The following is a brief description of the components and operations of the control and instrumentation system. More complete details may be found in Appendix D.

Microprocessor and Controller

A Rockwell International Inc. AIM 65/40 microcomputer forms the heart of the data acquisition and control system (Figure 10). The Central Processor Unit (CPU) will monitor the status of the following variables:

- tide
- pump flow rate
- pump discharge pressure
- motor current and voltage
- pneumatic air supply pressure

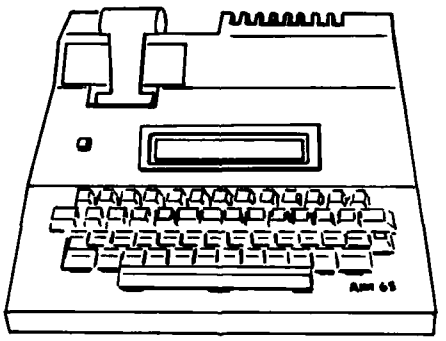

Figure 10. Schematic diagram of AIM 65/40 microcomputer.

The CPU will also control a bank of solenoid-actuated air valves that are individually connected to the 66 water valves via plastic tubing. During operation, should the CPU detect a pump or valve malfunction, the pump will be automatically stopped and the error recorded on a printer that is integral to the AIM 65/40. The printer will also be used to record normal system operation so that a complete operational record will be kept. As an added measure of detection, when a malfunction occurs, an alarm annunciator will be activated at Public Works, MINSY and an error message will be sent to NCEL via telephone.

Interfaces

In order for the microcomputer to receive and transmit information, an INTERSIL RAMDAC interface is used. This interface consists of several components described as follows:

a. RS232C Serial Interface Card. The RS232C card contains a conventional UART, a baud-rate generator, control and sequencing logic, and buffer registers. These allow the receiver/transmitter card to be easily interfaced from the remote station serial bus without additional support.

b. Receiver/Transmitter Board. The INTERSIL RAMDACS receiver/transmitter is a parallel-to-serial, serial-to-parallel interface, which provides the necessary link between the host computer (AIM 65/40) and the remote station serial bus.

c. Remote Digital Station (RDS) The RDS provides 36 channels of digital input/output (I/O). There are 16 CMOS level inputs, 16 CMOS (2.75 mA drive), outputs, and 4 CMOS I/O lines that can be used as either inputs or outputs. The receiver/transmitter supplies the command messages and the remote station responds with either data or status. The RDS communicates with the host computer via a specialized high security, serial protocol with data and error detection status messages.

d. Four-Channel Relay Input and Output Card. The relay card, with override switch for each channel, provides four independent sealed relays for switching external loads, diagnostic input, and LED indicators.

Instrumentation

The following sensors are used to monitor system status and the tide level.

a. The flow rate within each leg of the manifold pipe will be monitored via an ultrasonic clamp-on flow meter, model system 480, manufactured by Controlathon Inc. This meter measures the transit time of a sonic pulse and converts this measurement to an equivalent flow rate.

b. Two Viatron Inc., Model 501, pressure transducers will be used to sense the pump discharge pressure and the air supply pressure to the solenoid-actuated air valves. Output from the pressure transducers is 4 to 20 mA.

c. An Ohio Semitronics, Inc., Model OC9-99, AC power factor, watts, and VA transducer will provide a measurement of the real power, the apparent power, and the power factor in the 336-kW (450-hp)/480-volt pump motor.

d. The tide will be sensed using a Viatron Corp. submersible pressure transducer, Model 318M20. Output from the transducer will be 4 to 20 mA.

TEST PLAN

As discussed earlier, the object of the test bed scour jet array is to systematically verify Equations 1 and 2. In addition, the jet array test program will seek to explore the time rate of scour of the mud as a

function of the induced shear stress. The results will be used to determine the optimum shear stress and jet duty cycle with which to design an operational scour jet array.

The above objectives will be accomplished by conceptually splitting the array into three sections. Details of each section are contained in Table 1 and are discussed below.

Section 1 contains 27 jets and will be used to test the scouring ability of near-horizontal bottom-mounted jets with different diameters and flow rates. These jets will be operated in groups of 1, 3, 6, and 15 jets to produce nominal scour radii of 30, 20, 15, and 10 meters (98, 66, 49, and 33 feet), respectively. All of the jets will have duty cycle times of 12 minutes. They will also be near-horizontal (5-degree jet angle) and mounted as close to the bottom as possible. Because of the structure of the toe of the quay wall, the jets will actually be 2.59 meters (8.5 feet) above project dredging depths (-10.4 meters (-34 feet) MLLW).

Section 2 will contain 21 jets and will be used to explore the effects of different duty cycle times. As with Section 1, all of the jets will be near-horizontal (5 degrees) and 2.59 meters (8.5 feet) above the bottom. All of the jets will be operated in groups of three. Based on Equation 1, the nominal scour radii are expected to be 20 meters (66 feet). Jet cycle times for each set of three jets will be 1.5, 3, 6, 12, 24, and 48 minutes, twice per day. A single set of three jets will be operated for 12 minutes once per day.

Section 3 will contain 18 jets at different heights and angles. This section will be used to verify Equation 2. Jets in this section will be operated in groups of three with 12-minute duty cycle times. The jet heights will be 3.35 and 4.27 meters (11 and 14 feet) relative to the project dredging depth. The jet angles will vary from 5 to 30 degrees relative to the horizontal. Details of these configurations may be found in Table 1.

Operating times for Sections 1, 2, and 3 are 72, 106.5, and 72 minutes, respectively, per tidal cycle. The total operating time for the array will be 4 hours 10.5 minutes per tidal cycle.

The typical test period for the array at MINSY will be from December through June. Under normal conditions, this is the period of maximum sedimentation and one in which the array should be operated daily.

One of the most critical elements of the test plan will be monitoring of the scour performance of the jet array. It is recommended that monitoring be accomplished by monthly fathometer surveys. These surveys should be conducted using the procedures outlined in Jenkins et al. (1981).

Another critical element of the test plan will be maintenance and repair of the jet array. It is recommended that following each survey the jet array be inspected for malfunctions including the valves, pump, and control system. In most cases this may be done by inspecting the status of the valves (they should all be closed when not operational) and inspecting the data log tape on the controller.

Preventive maintenance of the system should be performed on a regular basis, possibly by MINSY personnel. Repair of the system during the test period will be the responsibility of NCEL and will be performed in-house or by contract.

ACKNOWLEDGMENTS

R. J. Tinsley was responsible for the design of the control system and instrumentation while J. Thayer and H. Kusano assisted in the mechanical design and performed all of the drafting.

REFERENCES

Ariathurai, R., and K. Arulanandan (1972). "Erosion rates of cohesive soils," American Society of Civil Engineers, Journal of the Hydraulics Division, vol 104, no. HY2, 1972, pp 279-283.

Arulanandan, K. (1975). "Fundamental aspects of erosion of cohesive soils," American Society of Civil Engineers, Journal of the Hydraulics Division, vol 101, no. HY5, 1975, pp 635-639.

Bailard, J. A. (1979). A design procedure for a scour jet array, Civil Engineering Laboratory, Technical Note N-1589. Port Hueneme, Calif., Sep 1979.

Gularte, R. C. (1978). Erosion of cohesive soils as a rate process, Ph D thesis, University of Rhode Island. Wakefield, R.I., 1978.

Jenkins, S. A., D. L. Inman, and W. G. Van Dorn (1981). The evaluation of sediment management procedures, Phase IV-VI final report, 1978-1980, Scripps Institution of Oceanography, Reference Series No. 81-22. La Jolla, Calif., 1981.

Malloy, R. J. (1980). U. S. Navy harbor maintenance dredging atlas, Civil Engineering Laboratory, Technical Note N-1597. Port Hueneme, Calif., Dec 1980.

Partheniades, E. (1965). "Erosion and deposition of cohesive soils," American Society of Civil Engineers, Journal of the Hydraulic Division, Proceedings paper 4204, 1965, pp 105-138.

Van Dorn, W. G., D. L. Inman, and S. McElmury (1975, 1978). Evaluation of sediment management procedures; Phase I, II and III, final report, 1974-75, 1975-76, 1976-77, Scripps Institution of Oceanography, Reference Series Nos. 75-32, 77-10, 78-18. La Jolla, Calif., 1975, 1978.

Vennard, J. K. (1963). Elementary fluid mechanics. New York, N.Y., John Wiley & Sons, 1963.

Table 1. Summary of Scour Jet Array Configurations

Section	Number of Jets	Jet Flow rate (m^3/sec)	Diameter (cm)	Height (m)	Angle (deg)	Time (min)	Nominal Scour Radius (m)
1	15	0.0253	3.38	2.59	5	12	10
1	6	0.0632	5.37	2.59	5	12	15
1	3	0.126	7.59	2.59	5	12	20
1	1	0.379	13.1	2.59	5	12	30
1	1	0.379	13.1	2.59	5	12	30
1	1	0.379	13.1	2.59	5	12	30
2	3	0.126	7.59	2.59	5	1.5	20
2	3	0.126	7.59	2.59	5	3	20
2	3	0.126	7.59	2.59	5	6	20
2	3	0.126	7.59	2.59	5	12	20
2	3	0.126	7.59	2.59	5	24	20
2	3	0.126	7.59	2.59	5	48	20
2	3	0.126	7.59	2.59	5	12[a]	20
3	3	0.126	7.59	3.35	5	12	20
3	3	0.126	7.59	3.35	15	12	23
3	3	0.126	7.59	3.35	30	12	23
3	3	0.126	7.59	4.27	5	12	21
3	3	0.126	7.59	4.27	15	12	18
3	3	0.126	7.59	4.27	30	12	16

[a]Once per day

Appendix A

A SUMMARY OF LABORATORY TESTS OF A SCOUR JET WITH VARIABLE HEIGHTS AND ANGLES

by

John Camperman
and
J. A. Bailard

INTRODUCTION

It has been proposed that sedimentation in berthing sites be controlled by removing freshly deposited sediment with fixed hydraulic jets. Model tests have previously been performed using horizontal near-bottom jets (Van Dorn et al., 1975), and limited full-scale tests have been conducted using raised and angled jets.

These studies have generated many questions regarding the effect of height and angle of the jet relative to the sediment plane. The study documented here investigated these questions by reproducing earlier model tests with the addition of variable jet heights and angles.

EXPERIMENTAL EQUIPMENT AND PROCEDURE

Equipment

The test bed was constructed from a 1.2 x 2.4-meter (4 x 8-foot) sheet of phenolic-coated plywood that was painted with black lines to provide a 0.051-meter (2-inch) grid over the entire sheet. A vertical aluminum rod, centered on one end of the sheet, supported a nozzle clamp that allowed vertical and angular adjustment of the nozzle (Figure A-1).

Experiments were conducted by lowering the test bed into a 3.7-meter-wide by 4.6-meter-long (12 x 15-foot) tank with the nozzle acting along the tank's longitudinal centerline and backed against one tank wall; this placed the nozzle tip 0.286 meter (0.782 foot) from the wall.

Following the work of Van Dorn (1975) a thin layer of diatomaceous earth (DE) was used to indicate the scour pattern by serving as an indicator of the 0.1-Pa (1.45×10^{-5}-psi) shear stress line. This method was used rather than making actual measurements of fluid shear stress. The effects of possible variations in the critical shear stress resulting from DE characteristics different from those used previously are discussed in ERROR ANALYSIS. In order to produce a controlled DE distribution a corral with a 0.15-meter- (0.5-foot-) high wall was constructed to temporarily fence the test bed during mixing and settling of the DE.

A Robins and Myers CDQ progressive cavity positive displacement pump, driven by a 3.7-kW (5-hp) motor with variable speed drive, provided controlled volumetric flow that was unaffected by changing inlet pressures at the nozzle. The test tank served as a reservoir from which freshwater was pumped to a flowmeter manifold, which then discharged through the nozzle. This manifold consisted of one 1.58×10^{-3} m^3/sec (25 gpm) and two 1.39×10^{-4} m^3/sec (2.2 gpm) rotameter type flowmeters for accurate control at a wide range of flow rates and included an air trap to eliminate bubbles from water flowing to the nozzle (Figure A-1).

The nozzle was connected to the manifold through a 0.019-meter (3/4-inch) flexible hose that terminated at a 0.0127-meter (1/2-inch), 90-degree elbow. A standard 0.0095- to 0.00635-meter (3/8- to 1/4-inch) threaded reducing bushing then attached the 0.10-meter- (4-inch-) long by 0.00991-meter (0.390-inch) smooth-bored tube, which served as the nozzle.

Procedure

Calibration. Flow rate was controlled by adjusting the motor drive speed and by valving the flow through the feedback leg flowmeters (Figure A-1) at low flow rates. Actual flow rates corresponding to

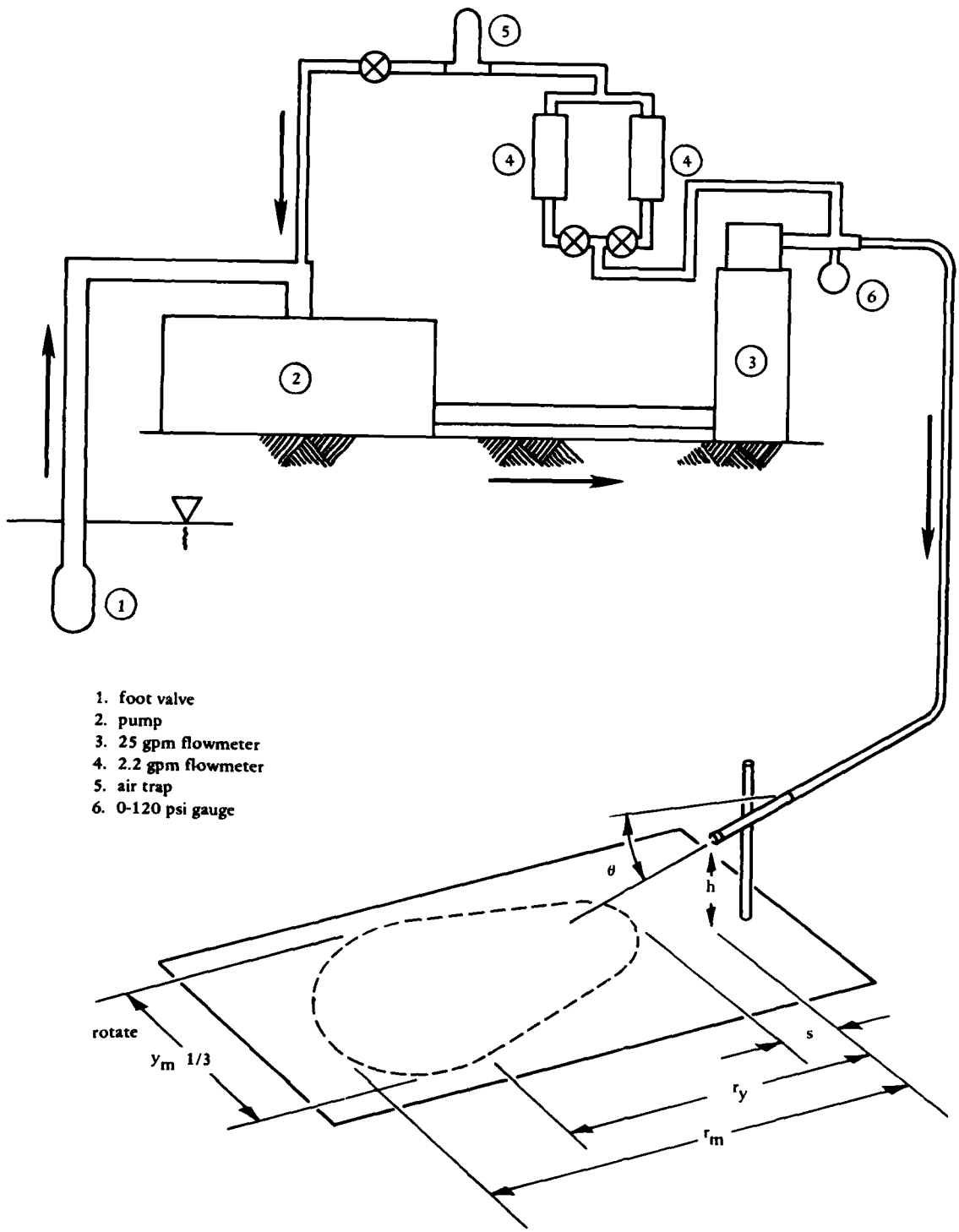

Figure A-1. Experimental apparatus.

flowmeter readings of 0.038, 0.126, 0.190, 0.253, 0.316, 0.380, 0.443, 0.506, 0.570, and 0.633 ℓ/sec (0.6, 2, 3, 4, 5, 6, 7, 8, 9, and 10 gpm) were determined by measuring the time needed to fill a known volume. All readings were within 0.19 ℓ/sec (0.3 gpm) of the actual flow rate, yet the actual flow rates were used in all data evaluation.

General Test Procedure. Water depth was adjusted to 0.915 meter (3 feet) above the test bed for all tests except those seeking to duplicate the results of Van Dorn et al. (1975). In order to duplicate conditions of previous scour experiments (Van Dorn et al., 1975) 0.345 liter (0.091 gallon) of diatomaceous earth was mixed with 3 liters (0.793 gallon) of water to produce a slurry. After raising the test bed with an overhead hoist until the corral wall just broke the water surface, the slurry was mixed in the water contained by the corral and allowed to settle. This produced a relatively uniform film of diatomaceous earth over the test bed with a concentration of 0.116 ℓ/m^2 (0.0028 gal/ft^2). The bed was then slowly lowered to the tank floor and the corral removed.

The tests were initiated by activating the pump to produce 0.038 ℓ/sec (0.6 gpm) flow and maintaining this flow for 10 minutes. Measurements of maximum scour radius (r_m), maximum scour width (y_m), radius to maximum width (r_y), and touchdown distance (s) were than made by reading the exposed grid lines of the test bed. This procedure was repeated for greater flow rates to produce progressively larger scour patterns with flows of up to 0.63 ℓ/sec (10 gpm); a photograph of the scour was taken for the 0.506-ℓ/sec (8-gpm) case.

The above procedure was conducted for a number of different nozzle heights and angles with a fresh deposit of diatomaceous earth for each nozzle configuration.

Depth Effect Test. To ensure that the jet plume was not affected by water depth and to allow comparison of results with previous work, the nozzle was directly attached to the test bed, giving it a horizontal orientation with centerline 0.0127 meter (0.5 inch) above the bed. Scour patterns were then generated using the previously described methods with water depths of 0.182 meter (0.6 foot) and 0.89 meter (2.92 feet).

Backing Wall Effect Test. Because the relative distance from the nozzle tip to the backing wall (24 nozzle diameters) was larger than that expected in the prototype, a test was conducted to investigate the effects of a closer backing wall. To achieve this a 0.61 x 0.46-meter (2 x 1.5-foot) rigid plastic sheet was secured to the nozzle support with the nozzle protruding through a hole in its center, producing a vertical backing wall 0.0172 meter (0.68 inch) or 1.7 nozzle diameters from the nozzle tip. Tests were then conducted using a nozzle height of 0.15 meter (0.492 foot) and a jet angle of 15 degrees.

RESULTS

Reproduction of Previous Experiments

Data acquired for the bottom-mounted horizontal nozzle are shown in dimensionless form in Figure A-2, following the format of Van Dorn et al. (1975). A critical shear stress, τ, of 0.1 Pa (0.145×10^{-4} psi)

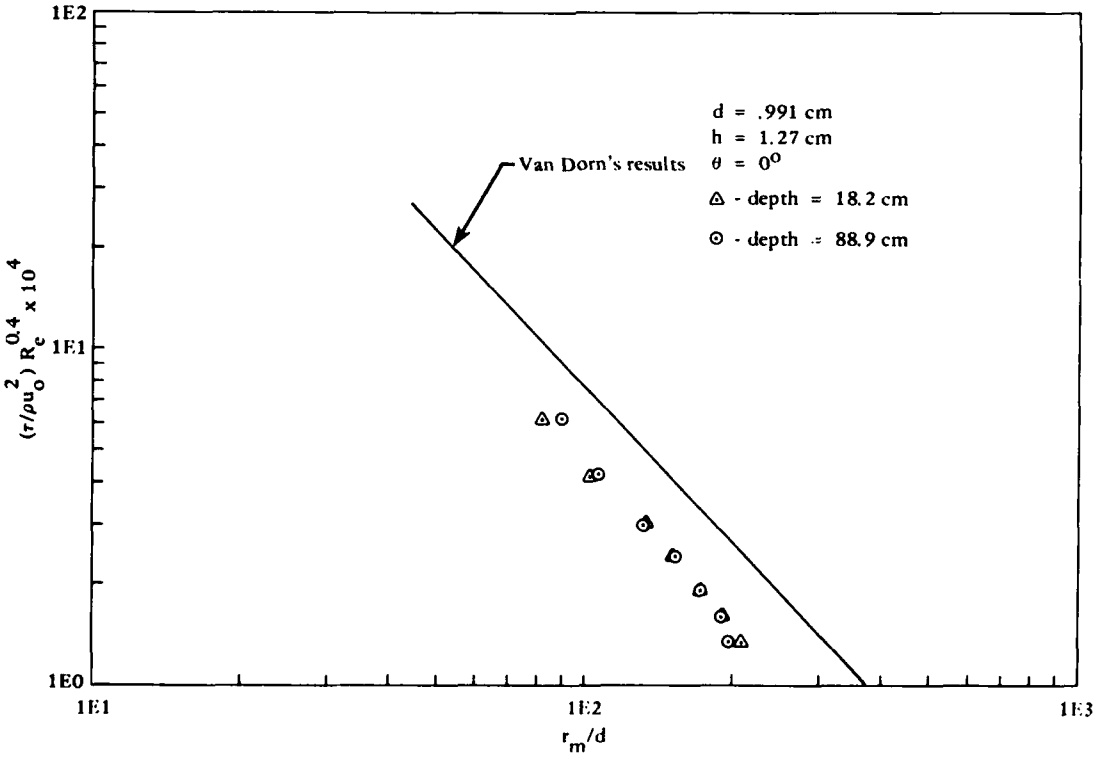

Figure A-2. Effects of water depth on the maximum scour radius, σ_m, as well as a comparison to the results of Van Dorn, et al., 1975.

was assumed for diatomaceous earth as this was the value reported by Van Dorn et al. (1975) using a stress probe. All water property values were based on freshwater at 21°C (70°F). It may be seen that the scour distance equation,

$$\frac{r_m}{d} = \left(\frac{\tau \, R_e^{0.4}}{120 \, \rho \, u_o^2} \right)^{-0.417} \qquad \text{(A-1)}$$

where ρ = fluid density

u_o = jet velocity

R_e = Reynolds number

d = jet diameter

r_m = scour radius

presented by Van Dorn et al. (1975) has been only partially reproduced. That is, the data are linear on the log-log plot with approximately the same slope, but there is a constant offset in the data which yields smaller scour distances for all flow rates. Thus the exponent -0.417 has been verified, but the combination of constants τ, ρ, and kinematic viscosity (υ) does not match Van Dorn's parameters. This difference is probably due to the actual shear stress (τ) of the present experiment being somewhat higher than the assumed value of 0.1 pa (1.45×10^{-4} psi) as discussed under ERROR ANALYSIS.

Water Depth Effects

It may be seen in Figure A-2 that varying the water depth from about 18 diameters above the nozzle to 90 diameters above the nozzle had little effect on scour range. It appears that at higher flow rates shallow water may amplify the scour range by narrowing the plume in the vertical plane, but since water depths required to produce this effect are well below prototype limits, this trend was not investigated further.

Scour Pattern Geometry

Scour pattern geometries for all nozzle configurations tested are shown in Figures A-3 through A-9 as four measurements, r_m, r_y, y_m, and s (Figure A-1), which are made nondimensional using the nozzle diameter. While these figures may themselves be used to predict scour geometry in full scale (using the proper τ, ρ, R_e), an attempt was made to describe scour dimensions as a function of nozzle configuration (d, θ, h), jet velocity (u_o), fluid properties (ρ, υ), and sediment shear stress (τ).

After an extended effort it was found that only the maximum scour range (r_m) behaved systematically enough to allow its representation as a single equation. This equation, shown below, is the result of employing a Chebychev curve fitting computer analysis to the data shown in Figures A-3 and A-4. The variation of the constants C_o, C_1, and C_2 as a function of nozzle height and angle was then analyzed and analytically modeled as follows:

$$\frac{r_m}{d} = \left(\frac{\tau \, R_e^{0.4} \times 10^4}{C_o \, \rho \, u_o^2} \right)^{C_1} \qquad \text{(A-2)}$$

$$C_o = 10^{(-C_2/C_1)}$$

$$C_1 = 0.0533 \sin (5.59\,\theta) - 0.385 + (-0.0201 + 0.00593\,\theta^{0.356}) \frac{h}{d}$$

$$C_2 = 2.442 + 0.0108 \frac{h}{d} - 1.266 \times 10^{-4} \left(\frac{h}{d}\right)^2 - 0.0118\,\theta + 9.33 \times 10^{-5}\,\theta^2$$

where the nozzle angle to the horizontal is measured in degrees. The bounds on the above equation are:

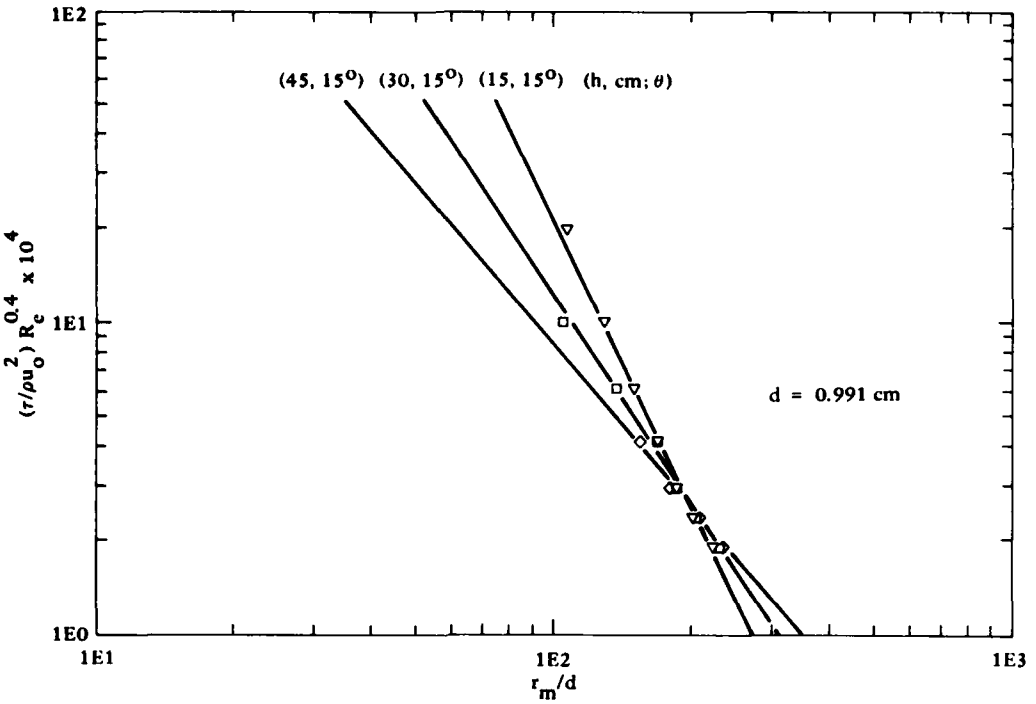

Figure A-3. Scour range (r_m) for small angle jets.

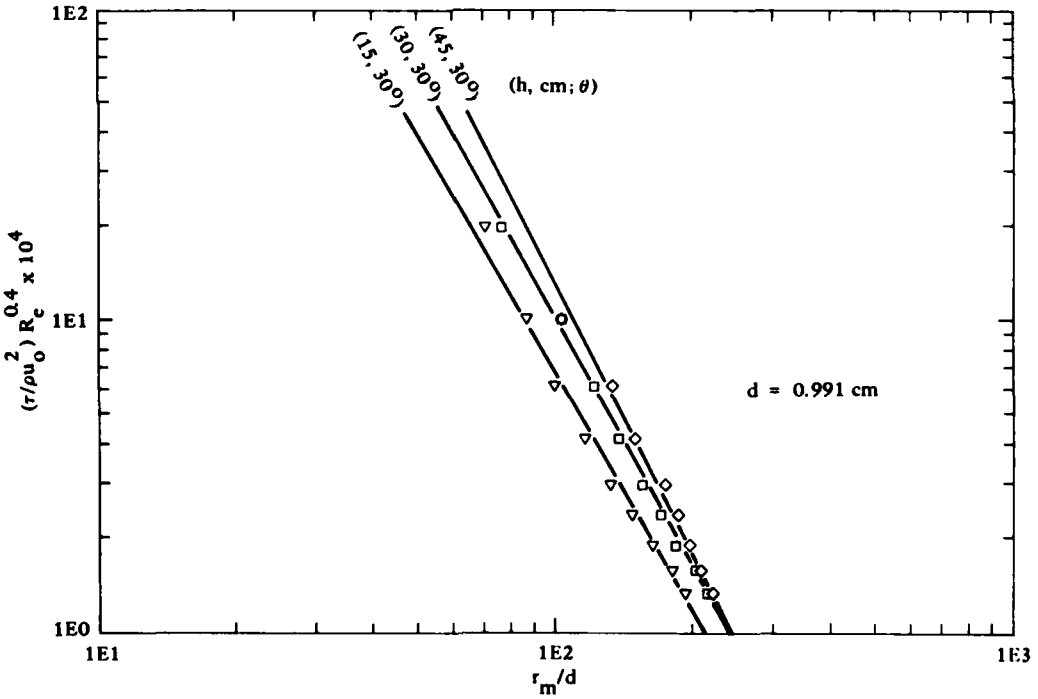

Figure A-4. Scour range (r_m) for large angle jets.

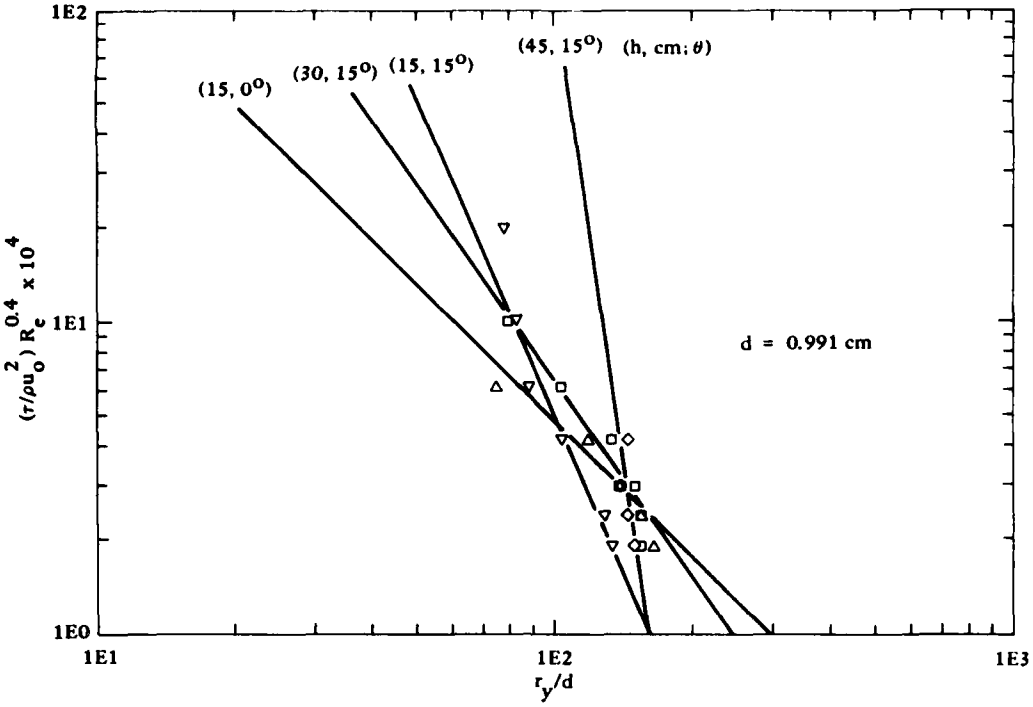

Figure A-5. Range to maximum scour width (r_y) for small jet angles.

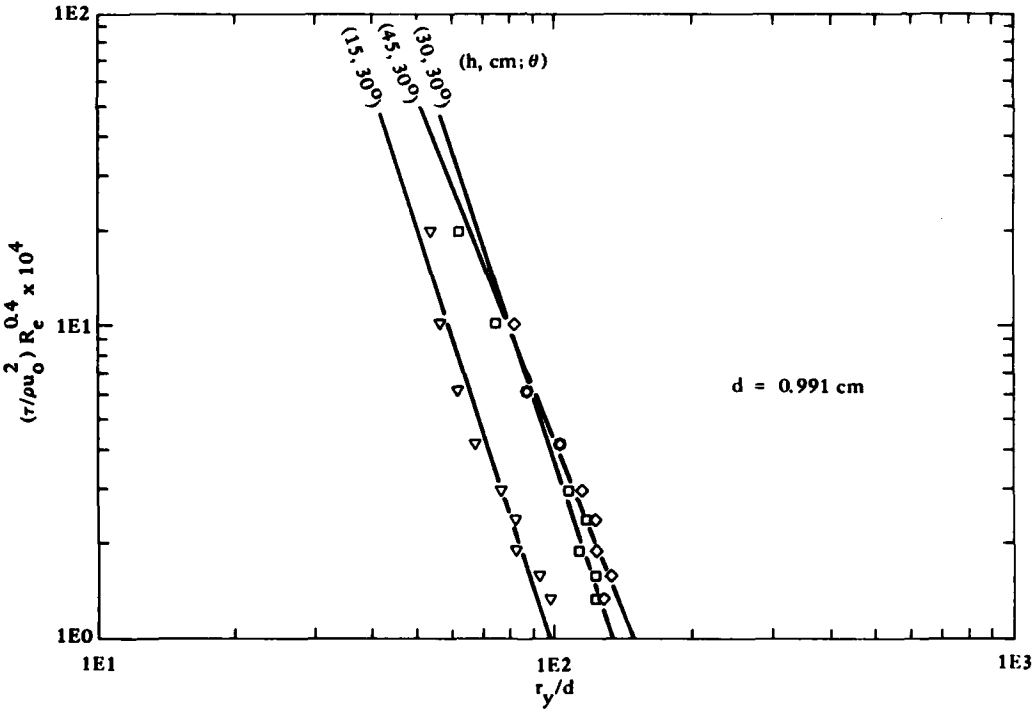

Figure A-6. Range to maximum scour width (r_y) for large jet angles.

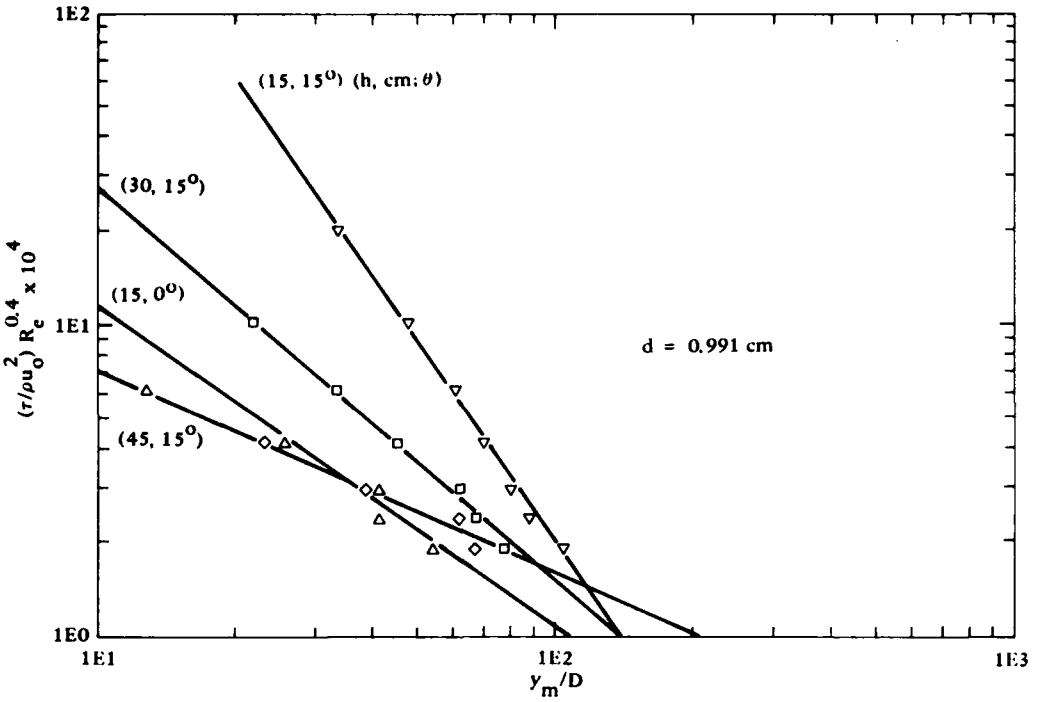

Figure A-7. Maximum scour width (y_m) for small jet angles.

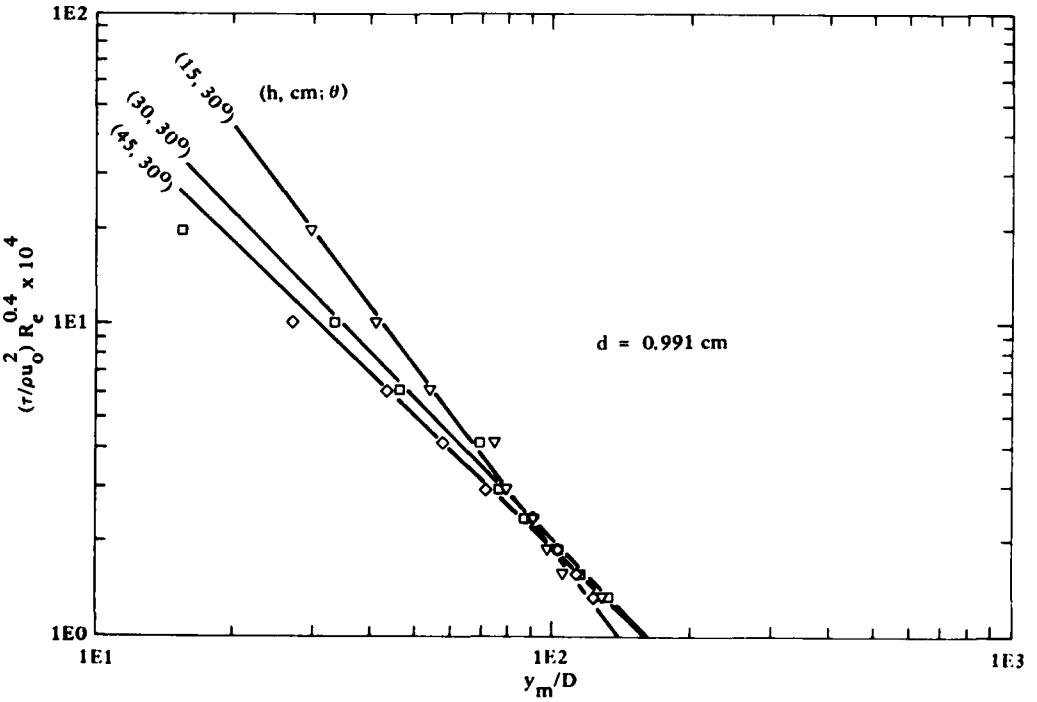

Figure A-8. Maximum scour width (y_m) for large jet angles.

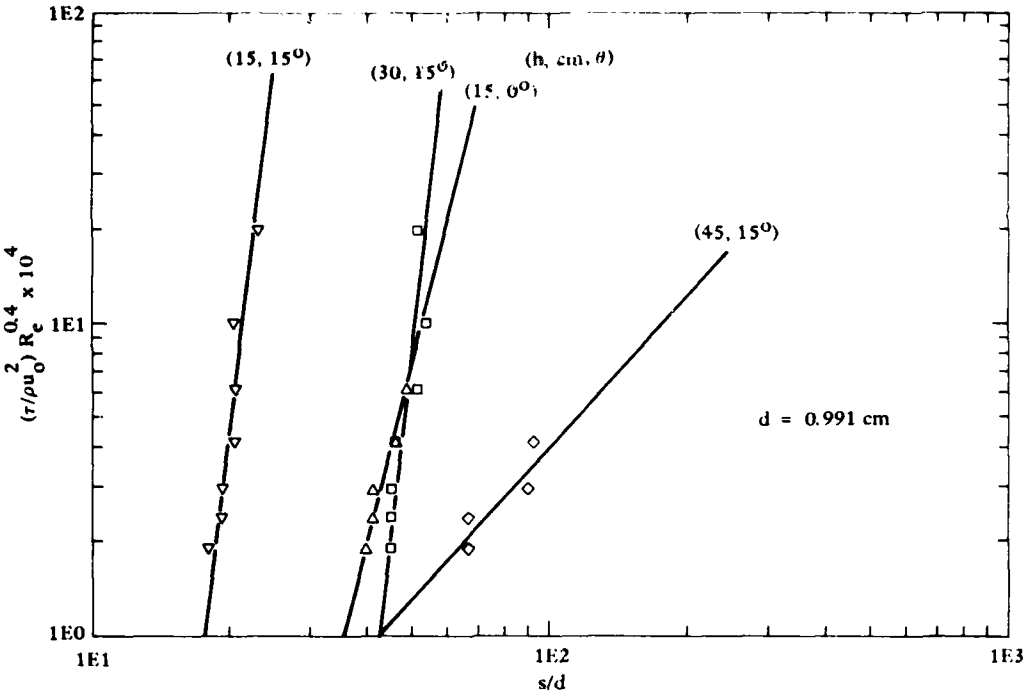

Figure A-9. Touch down distance (s).

$0 \leq \theta \leq 30^\circ$ and $1.28 \leq h/d \leq 45.4$,

excluding $\theta < 15$ degrees when $h/d > 15.1$

Backing Wall Effects

The results produced after changing the backing wall distance from the standard 24 nozzle diameters to a reduced 1.7 diameters with a nozzle configuration of $\theta = 15$ degrees and $h/d = 15.1$ are shown in Figure A-10. Here it is seen that for the closer wall, the scour distance is generally greater. This is probably due to the altering of streamlines of the water being entrained into the plume. This increase in radius is significant (up to 10%) and indicates that the present experiments with their large backing wall distances yield scour ranges that are less than that expected in the prototype where nozzles will be located relatively close to the backing wall.

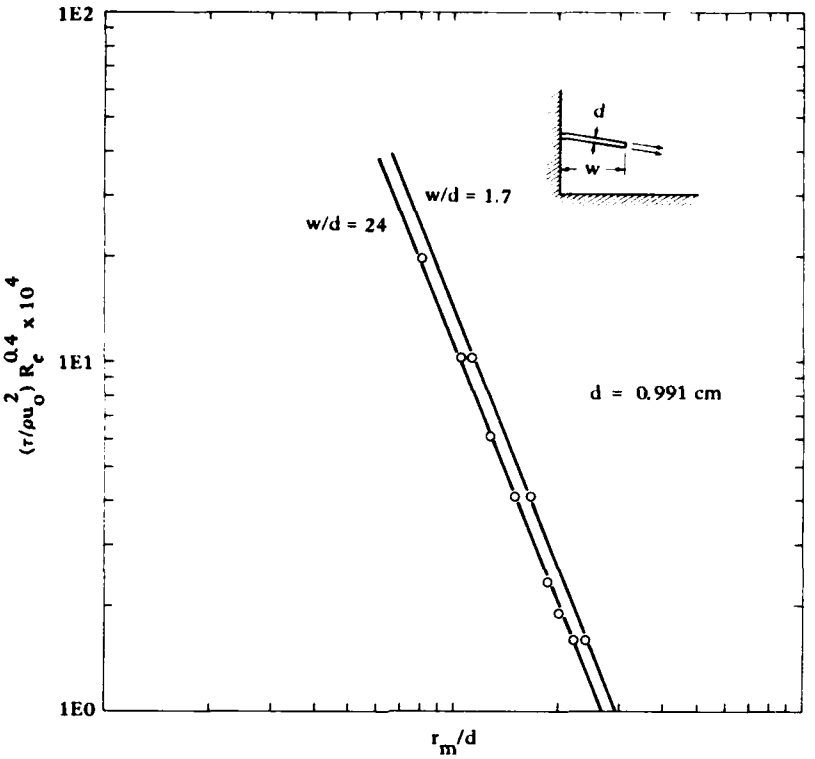

Figure A-10. Effect of changing backing wall distance (w) for h/d = 15, θ = 15°.

ERROR ANALYSIS

Reproduction of Previous Experiments

The discrepancy between the present results and those reported by Van Dorn et al. (1975) may be due to backing wall effects or to differing values of ρ, υ, and/or τ. It may be shown that varying the values of ρ and υ for freshwater between 10°C and 27°C (50°F and 80°F) produces less than half the measured discrepancy; thus, backing wall effects and the possibly different shear stress values necessary to produce scour are the most probable sources of the apparent difference between Van Dorn's and the present results.

Regarding the critical shear stress of diatomaceous earth, it was found that if this shear stress were assumed to be 0.167 Pa (2.42 x 10^{-5} psi) instead of 0.1 Pa (1.45 x 10^{-5} psi), the present experimental data would more closely match Van Dorn's work (Figure A-11). When the corrected value of shear stress is employed, Equation A-2 is altered only in the constant C_2 as follows:

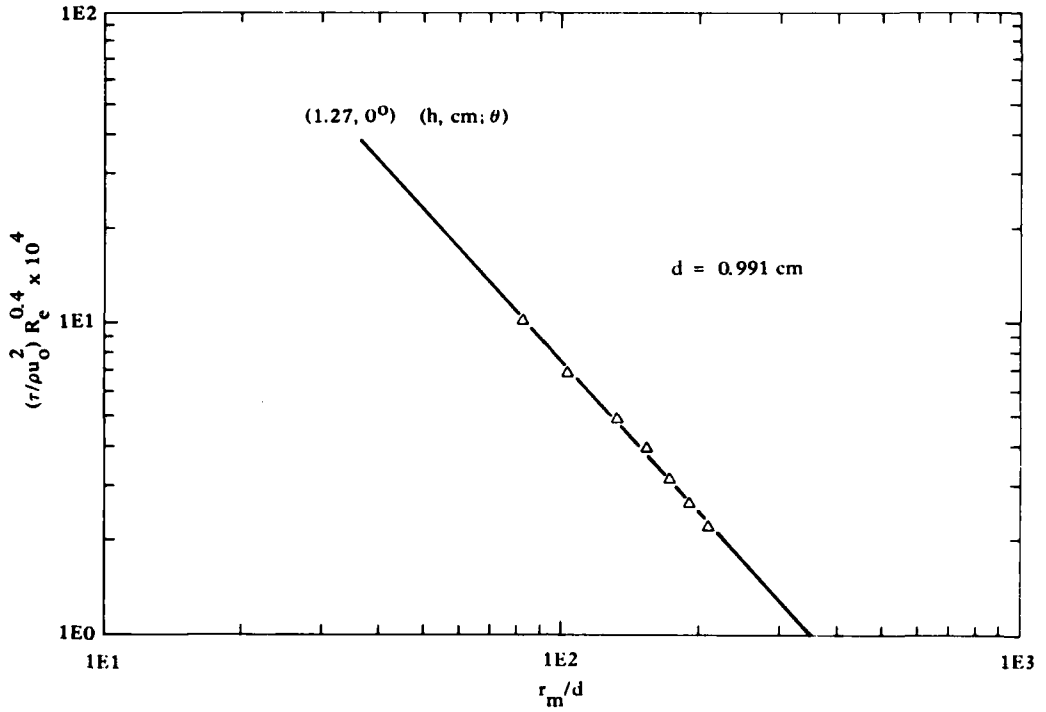

Figure A-11. Correction to data for shear stress at 1.67 dynes/cm^2.

C_2 corrected = 1.67 C_2

When using graphical presentations of the present data for predicting scour pattern dimensions, this correction is incorporated by multiplying the ordinate of a data point by 1.67; thus, any set of data for a given nozzle configuration may be shifted to be in agreement with the previous horizontal jet data (with no backwall).

Accuracy of Scour Radius Analytical Model

Within the experimental limits in the variables h/d and θ, Equation A-2 with C_2 corrected predicts the scour range to within 10% of the actual measured values for any nozzle configuration and has less than a 4% error for any nozzle configuration with h/d greater than 1.3.

Scour Plane Versus Scour Volume

It must be kept in mind that full-scale scouring will involve a soft bottom, which was not modeled by the rigid bed in this experiment. The soft bottom will produce a three-dimensional scour pattern, which will presumably be considerably different than that for a flat plate. For small nozzle angles, the modeling error is probably small, but as nozzle angle increases in the prototype a depression will be scoured which will cause the scour pattern to be smaller than the pattern created by the same jet impinging on a rigid, flat surface.

CONCLUSIONS AND RECOMMENDATIONS

The following conclusions were reached as a result of data analysis.

1. Data trends and patterns found in previous work (Van Dorn et al., 1975) have been reproduced. Absolute values remain unchecked due tc unknown wall effects and shear stress values required to scour DE.

2. An analytical model for predicting the maximum scour radius as function of jet discharge velocity, jet diameter, jet height, jet angle and mud characteristics has been derived.

3. The maximum width, radius to maximum width, and touchdown distanc of the scour pattern for variable nozzle heights and angles have be documented graphically.

4. The greatest maximum scour radius was achieved with low nozz heights and small downward angles at high flow rates.

In order to optimize the scour radius, it is recommen that jets be located slightly above the area to be scou and at a slight downward angle. It appears that the opti

position for high flow rate jets is at a height between zero and 15 nozzle diameters and at a downward angle between zero and 15 degrees.

The present experiment covered a broad range of nozzle configurations and indicates the optimum range discussed above. Additional testing to provide greater resolution at the low heights, small angles should be performed to provide more precise optimization of the nozzle geometry.

Further testing should be done to answer the remaining questions regarding the effects of shear stress value and backwall spacing to provide predictive relationships usable for design. The testing should include some full-scale field tests.

Appendix B

DESIGN DRAWINGS FOR THE JET ARRAY

The following Figures B-1 to B-7 are engineering design drawings for the test bed jet array.

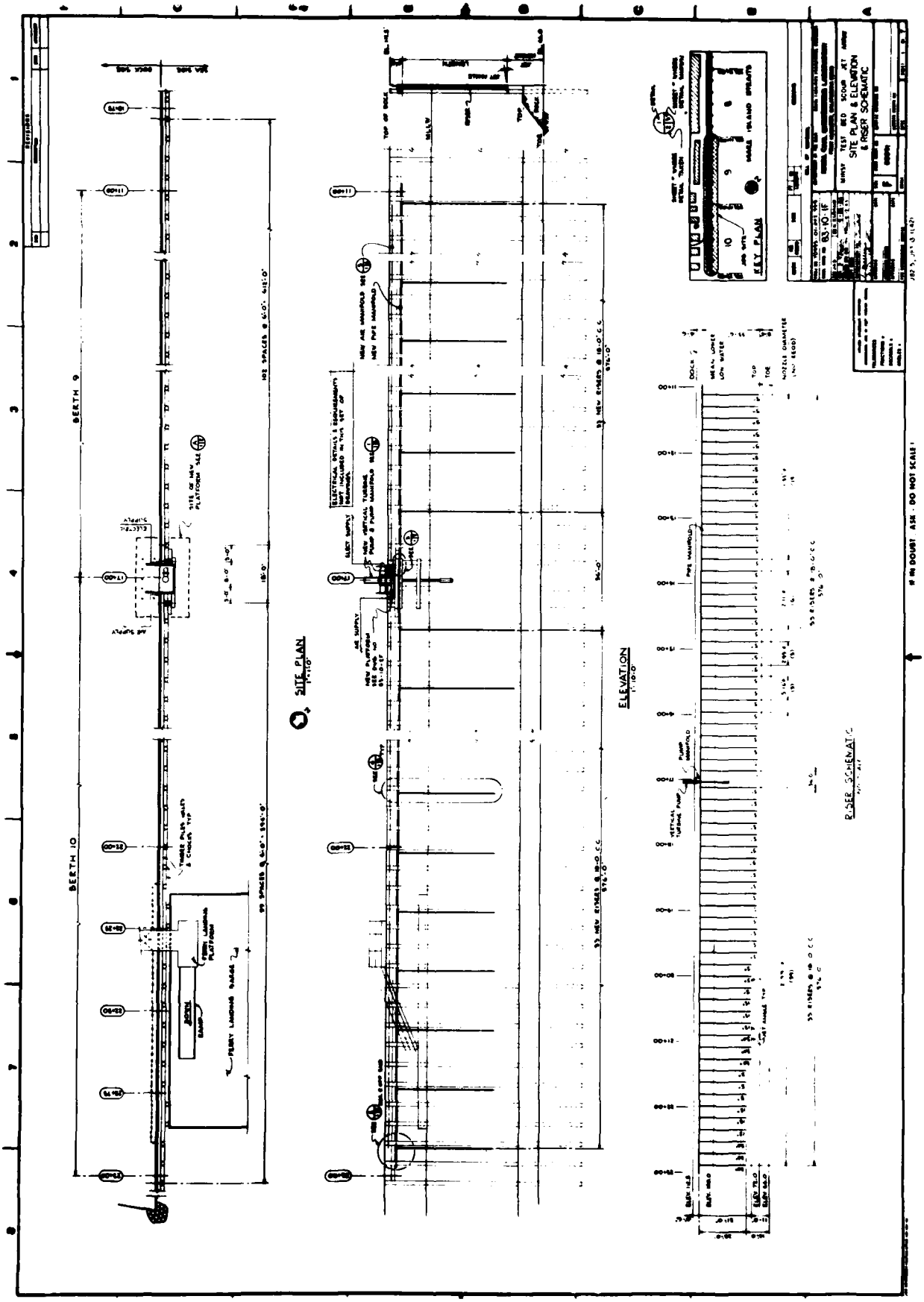

Figure B-1. Site plan, elevation and riser schematic.

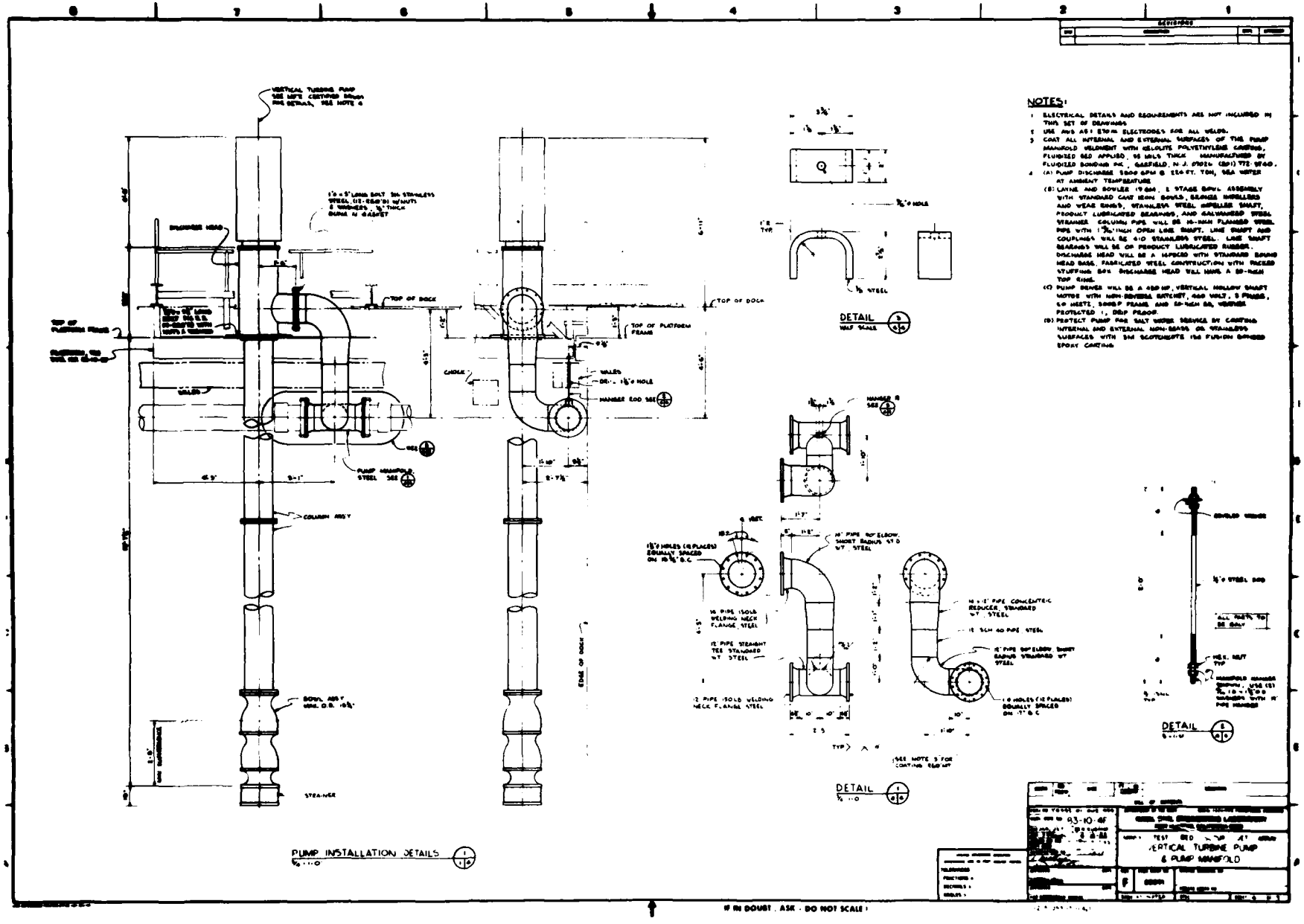

Figure B-2. Vertical turbine pump and pump manifold.

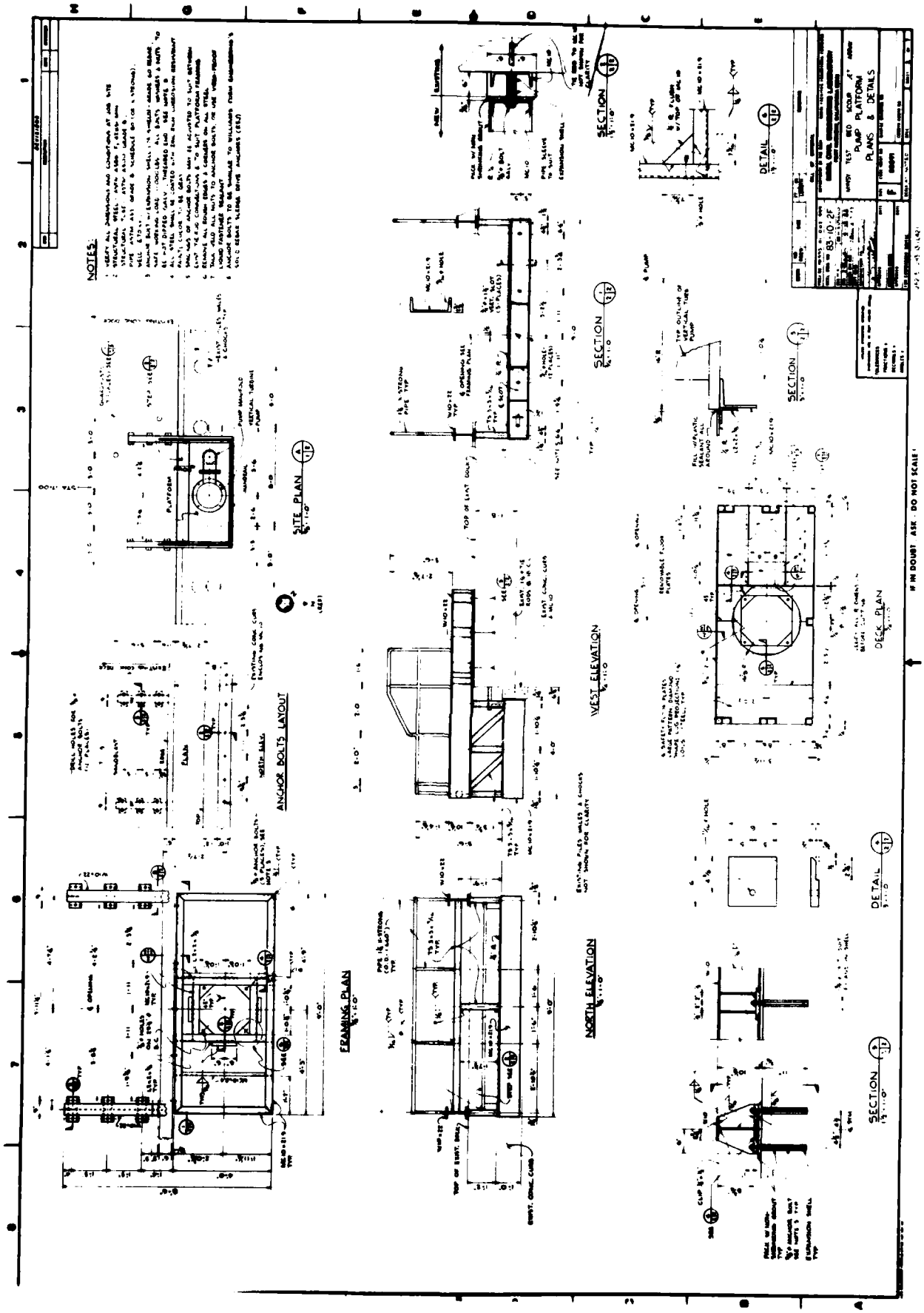

Figure B-3. Vertical turbine pump platform.

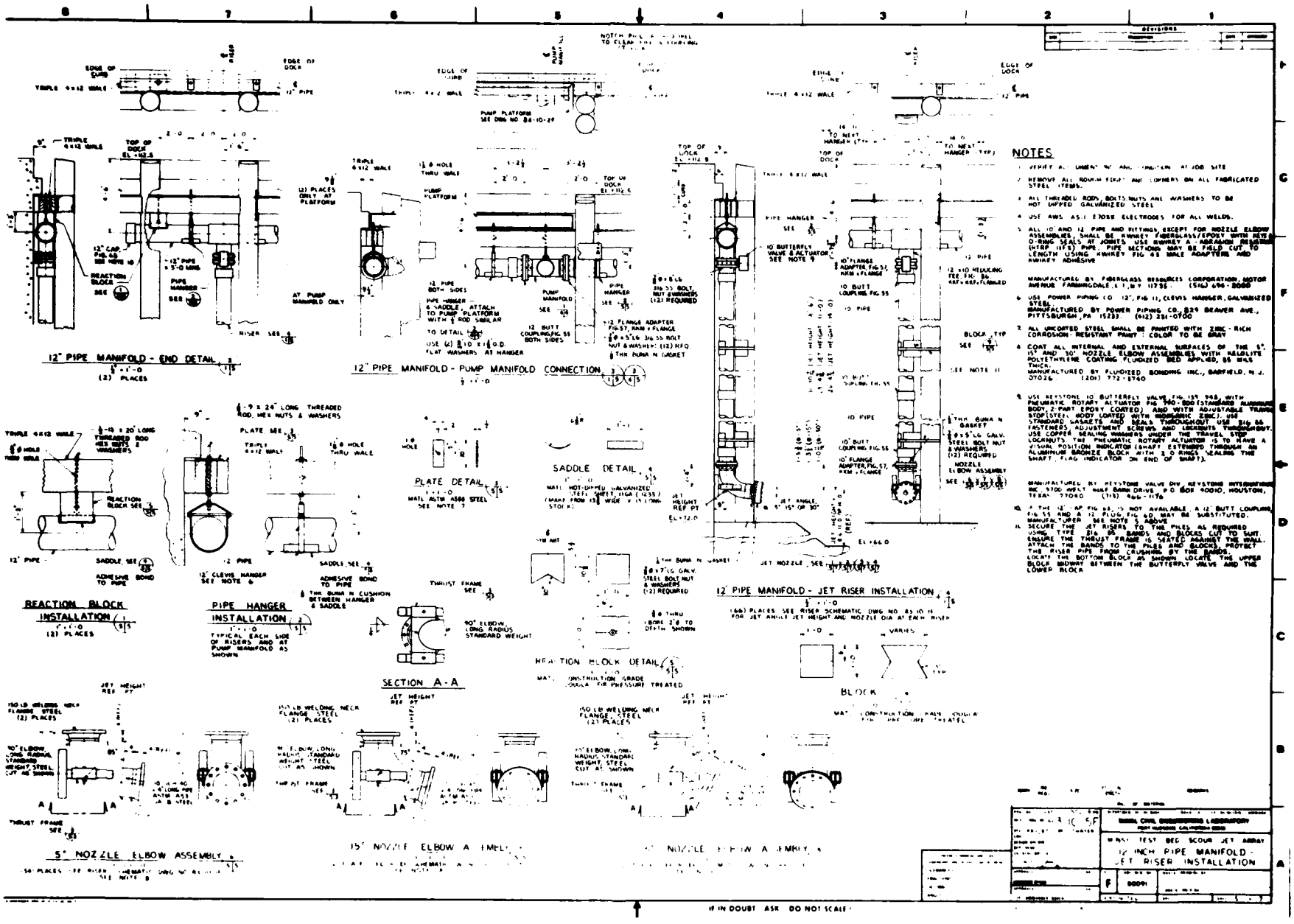

Figure B-4. Pipe manifold and jet riser installation.

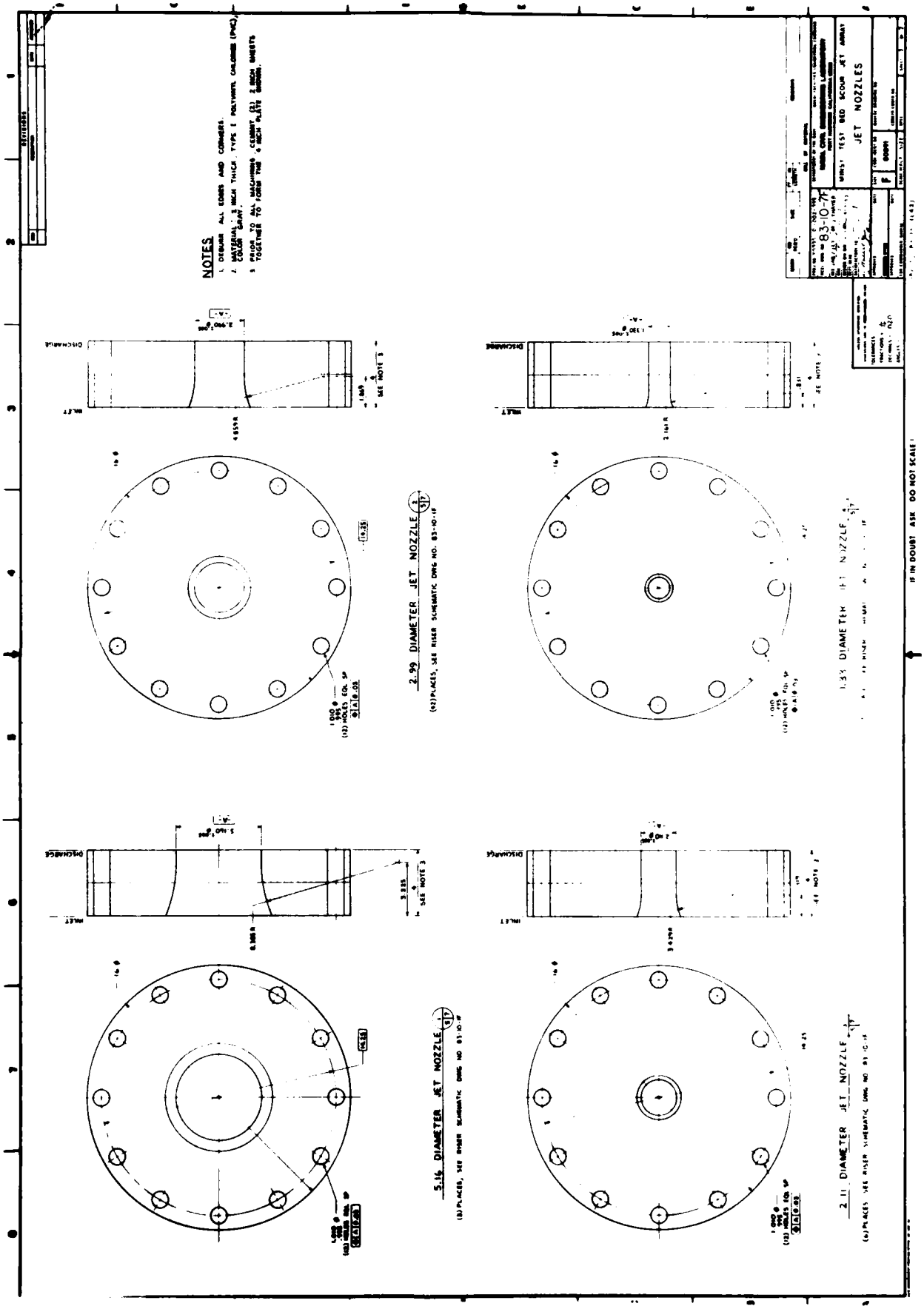

Figure B-5. Jet nozzle details.

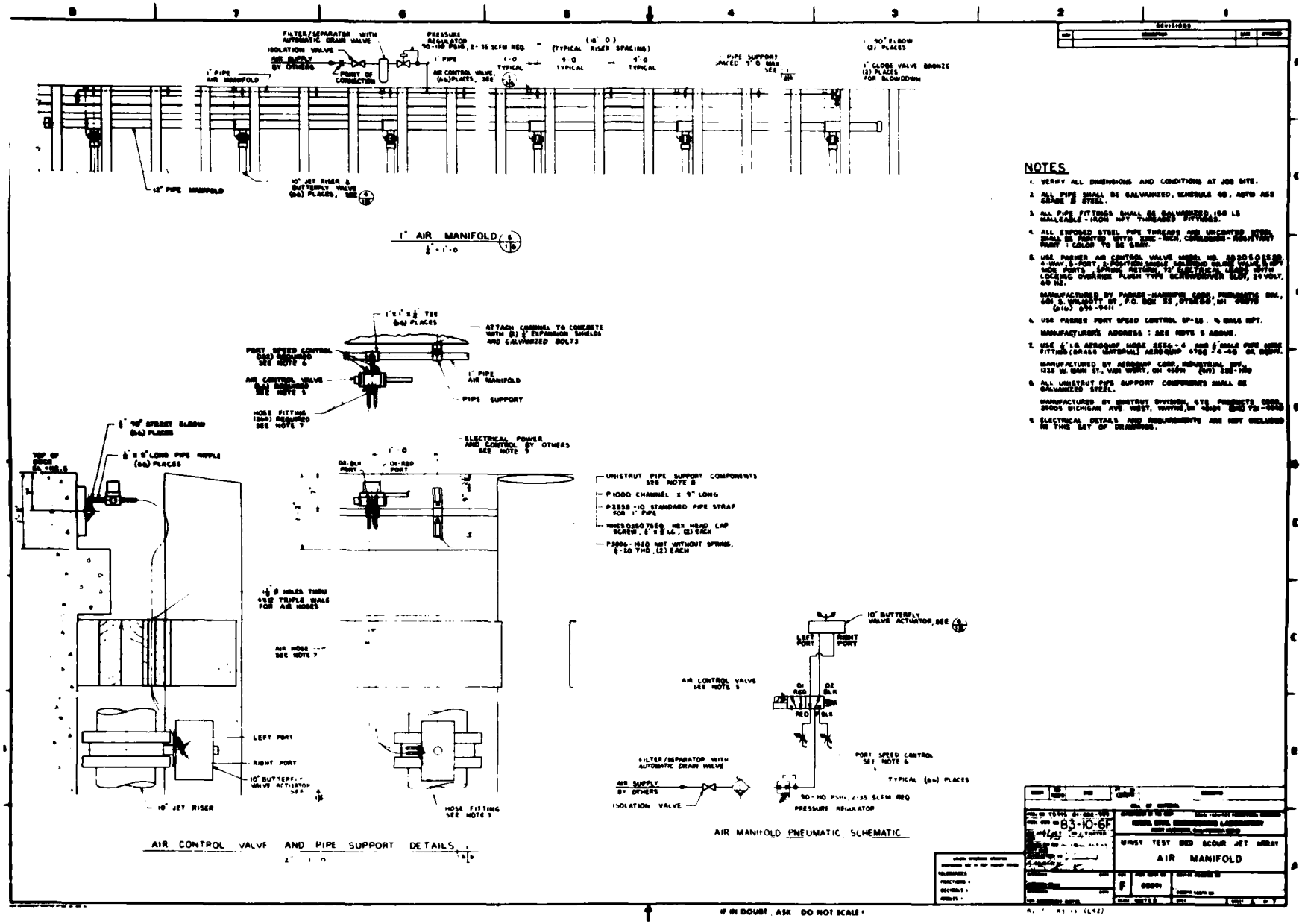

Figure B-6. Air manifold details.

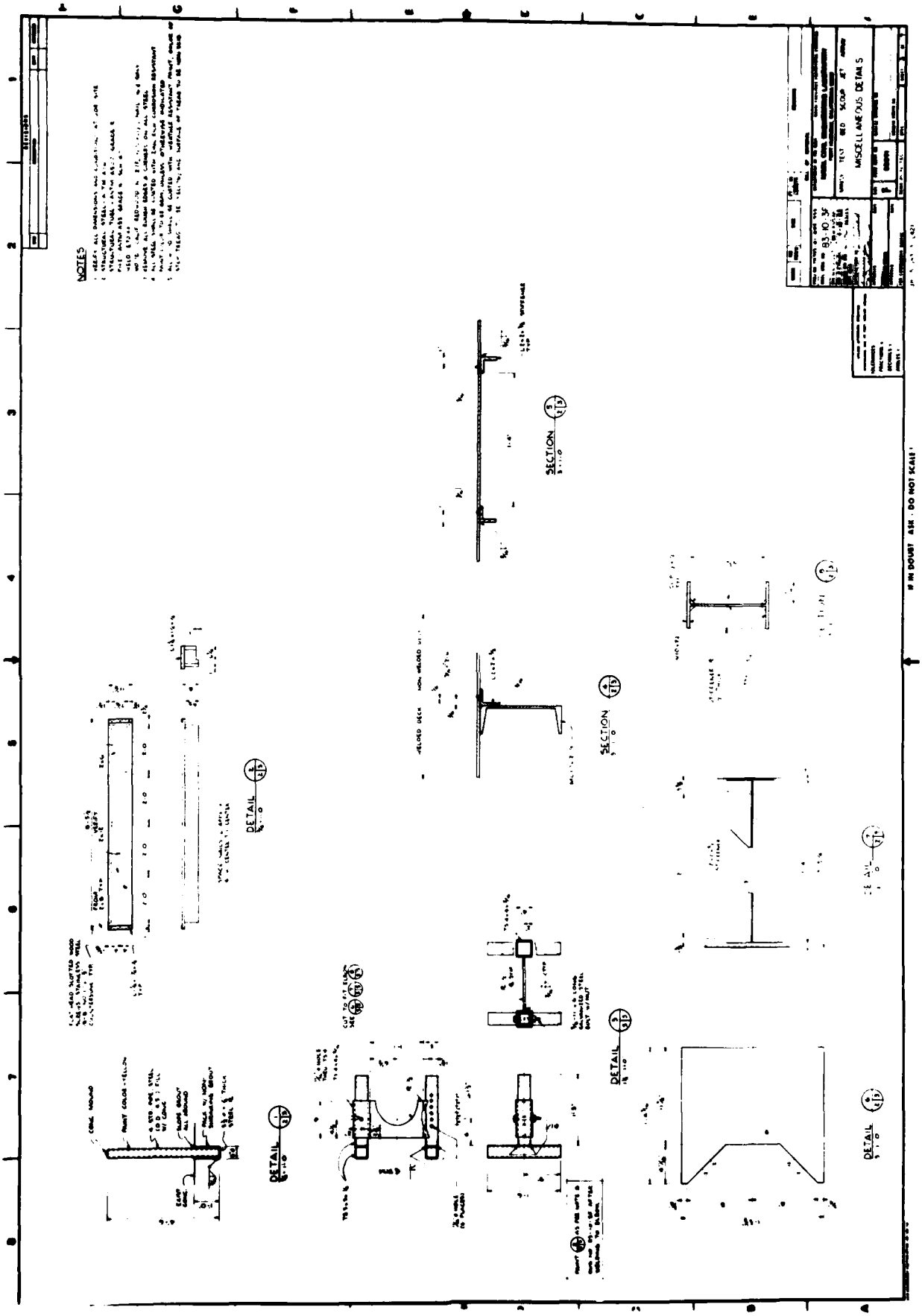

Figure B-7. Miscellaneous details.

Appendix C

DERIVATION OF AN EQUATION TO PREDICT THE OPTIMUM JET DIAMETER FOR A JET ARRAY SYSTEM WITH PREDETERMINED PIPING SIZES

For the case of a horizontal, bottom-mounted jet, the scour radius, r_m, is given by Equation 1, i.e.,

$$\left(\frac{r_m}{d}\right)^{2.4} = 120 \frac{\rho u_o^2}{\tau} \left(\frac{u_o d}{\upsilon}\right)^{-0.4} \tag{C-1}$$

where d is the jet diameter, u_o is the jet velocity, ρ is the fluid density, υ is the kinematic viscosity, and τ is the required shear stress. Rearranging the equation and substituting $Q = (\pi d^2/4)u_o$, one obtains

$$Q = \frac{\pi}{4} \left(\frac{\tau}{120 \rho \upsilon^{0.4}}\right)^{0.625} r^{1.5} d^{0.75} \tag{C-2}$$

Based on conventional pipe flow equations, the total dynamic head required of the pump, h_2, can be expressed as

$$h_L = \frac{8}{\pi^2 g} \left(C_1 + C_2 d^{-4}\right) Q^2 \tag{C-3}$$

where

$$C_1 = \sum\left(\frac{k_L}{D^4} + \frac{f \ell}{D^5}\right) \tag{C-4}$$

$$C_2 = \left(1 + k_{L\ nozzle}\right) \tag{C-5}$$

and k_L are the minor piping losses, D is the local pipe diameter, f is the friction factor, and ℓ is the pipe length under consideration. Finally, the power of the motor required to drive the pump, ω_{motor}, can be expressed as

$$\omega_{motor} = \rho\, g\, Q\, h_L/\eta \tag{C-6}$$

where η is the pump efficiency.

Combining Equations A2, A3, and A6, one obtains

$$\omega_{motor} = \frac{\pi}{8\eta}\left(\frac{\tau}{120\ \rho^{-467}\ \upsilon^{0.4}}\right)^{1.875} r^{4.5}\left(C_1 d^{2.25} + C_2 d^{-1.75}\right) \tag{C-7}$$

Finally, using Equation C-7 to calculate the optimum jet diameter that minimizes the required power, one obtains

$$d = \left(\frac{1.75\ C_2}{2.25\ C_1}\right)^{0.25} \tag{C-8}$$

Appendix D

CONTROL DRAWINGS AND INSTRUMENTATION

Figure D-1 shows a block diagram of the control and instrumentation system. Designated components are described in Table D-1.

Table D-1. Components for the Jet Array Control and Instrumentation System

Component	Description
A-1	Rockwell International Inc. AIM 65/40 Microcomputer Model No. A65/40
A-2	Intersil, Inc. REMDACS 11 Receiver/Transmitter Card Model No. REM-R/T-2
A-3	Intersil, Inc. REMDACS 11 RS232C Card Model No. SI-RS232
A-4	Rockwell International Inc. 2400 bps MOS/LSI Modem Model No. V96P/1
A-5	Rockwell International Inc. Power Supply With Battery Backup Model No. A65-004
T-1	Intersil, Inc. REMDACS 11 Remote Voltage Card Model No. REM24-V216
T-2, T-11 & T-15	Intersil, Inc. REMDACS 11, Remote Digital Card Model No. REM24-D210
T-3 through T-210 & T-12 through T-14 & T-16 through T-20	Intersil, Inc. REMDAC 11, Remote Four Channel Relay Card Model No. REM-DP-R204
Jet Valve No. 1 through 62	Humphrey Products Air Control Valves Model No.
S-1	Viatran Corp. Tide Sensor Submersion Pressure Transducer Model No. 318M20
S-2	Ohio Semitronics Inc. Three Phase K.W. Detector Model No. PC9-81
S-3 & S-4	Controlathon Inc. Ultrasonic Flowmeters Model System 480

Table D-1. Continued

Component	Description
S-5 & S-6	Viatran Corp. Pressure Transducer Model No. 501
S-7 & S-8	Alarms Inc. Error or Limit Alarm Modems Model No. 12
S-9	Square D. Company 480V/400 HP Pump Control Magnetic Contactor and Starter Model No. Class 8536 Size 8

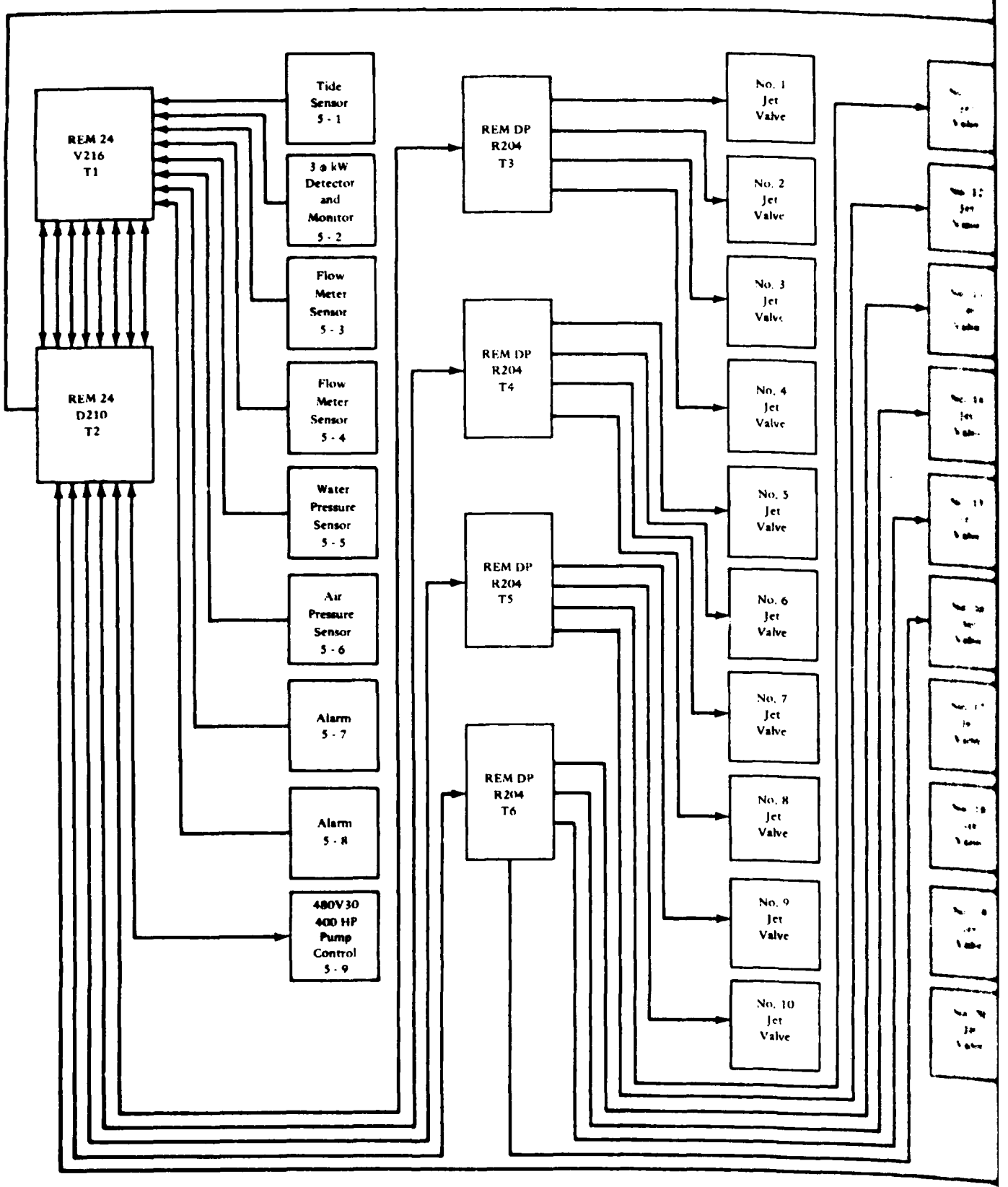
REM 24
V216
T1
REM 24
D210
T2
Tide
Sensor
5 - 1
3 @ kW
Detector
and
Monitor
5 - 2
Flow
Meter
Sensor
5 - 3
Flow
Meter
Sensor
5 - 4
Water
Pressure
Sensor
5 - 5
Air
Pressure
Sensor
5 - 6
Alarm
5 - 7
Alarm
5 - 8
480V30
400 HP
Pump
Control
5 - 9
REM DP
R204
T3
REM DP
R204
T4
REM DP
R204
T5
REM DP
R204
T6
No. 1
Jet
Valve
No. 2
Jet
Valve
No. 3
Jet
Valve
No. 4
Jet
Valve
No. 5
Jet
Valve
No. 6
Jet
Valve
No. 7
Jet
Valve
No. 8
Jet
Valve
No. 9
Jet
Valve
No. 10
Jet
Valve

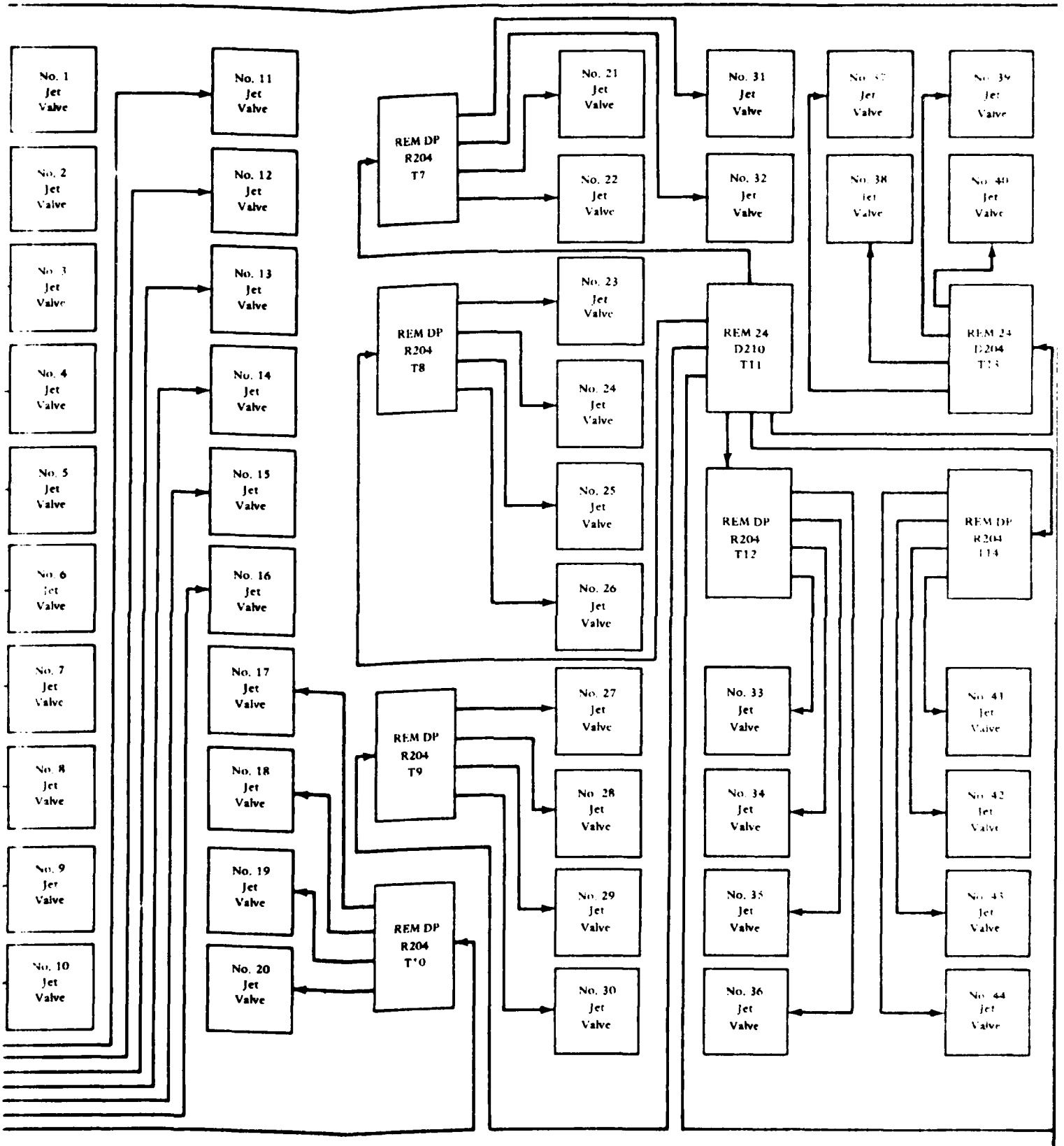

Figure D-1. Block diagram for control and instrumentation system

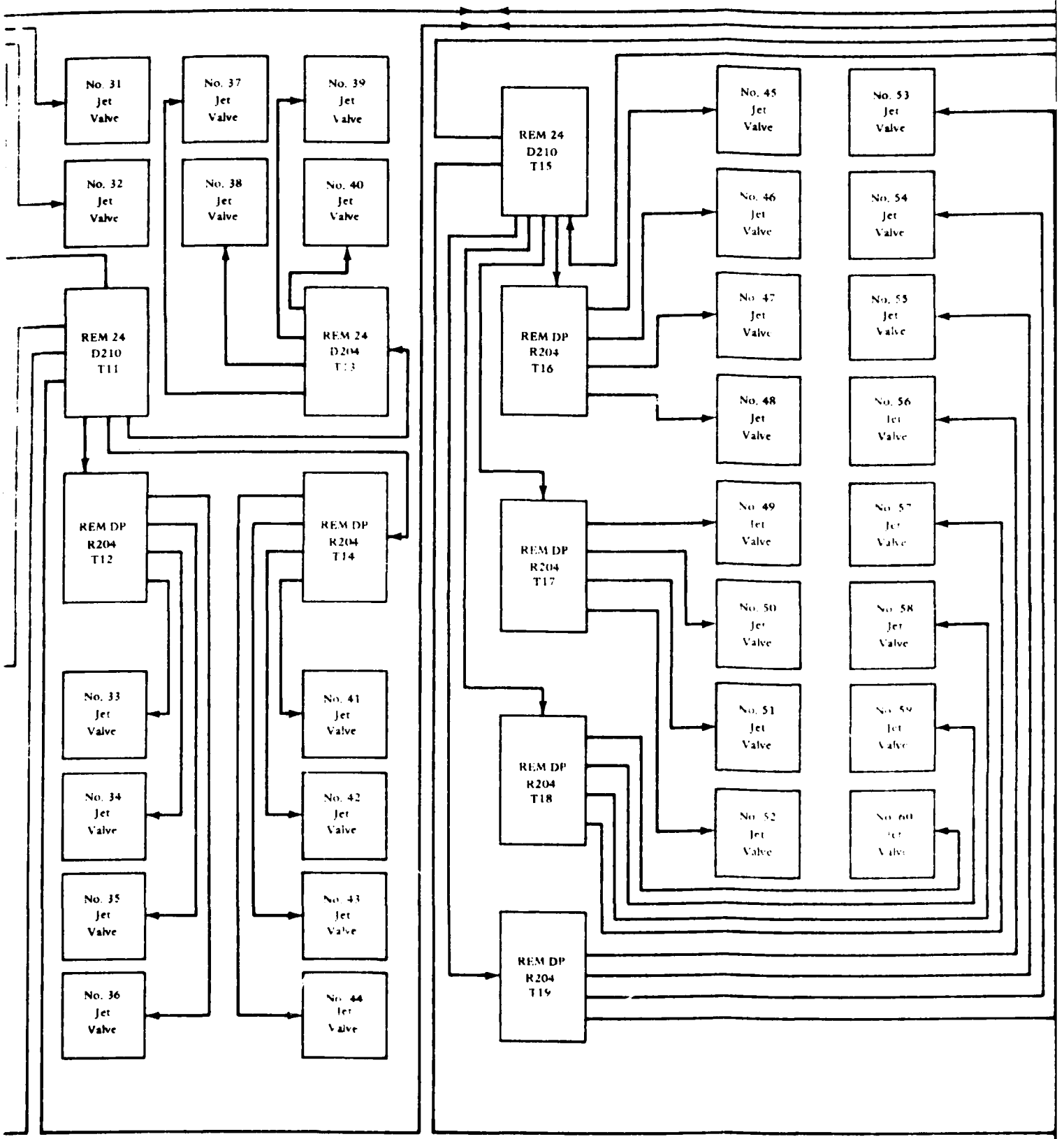

control and instrumentation system.

3

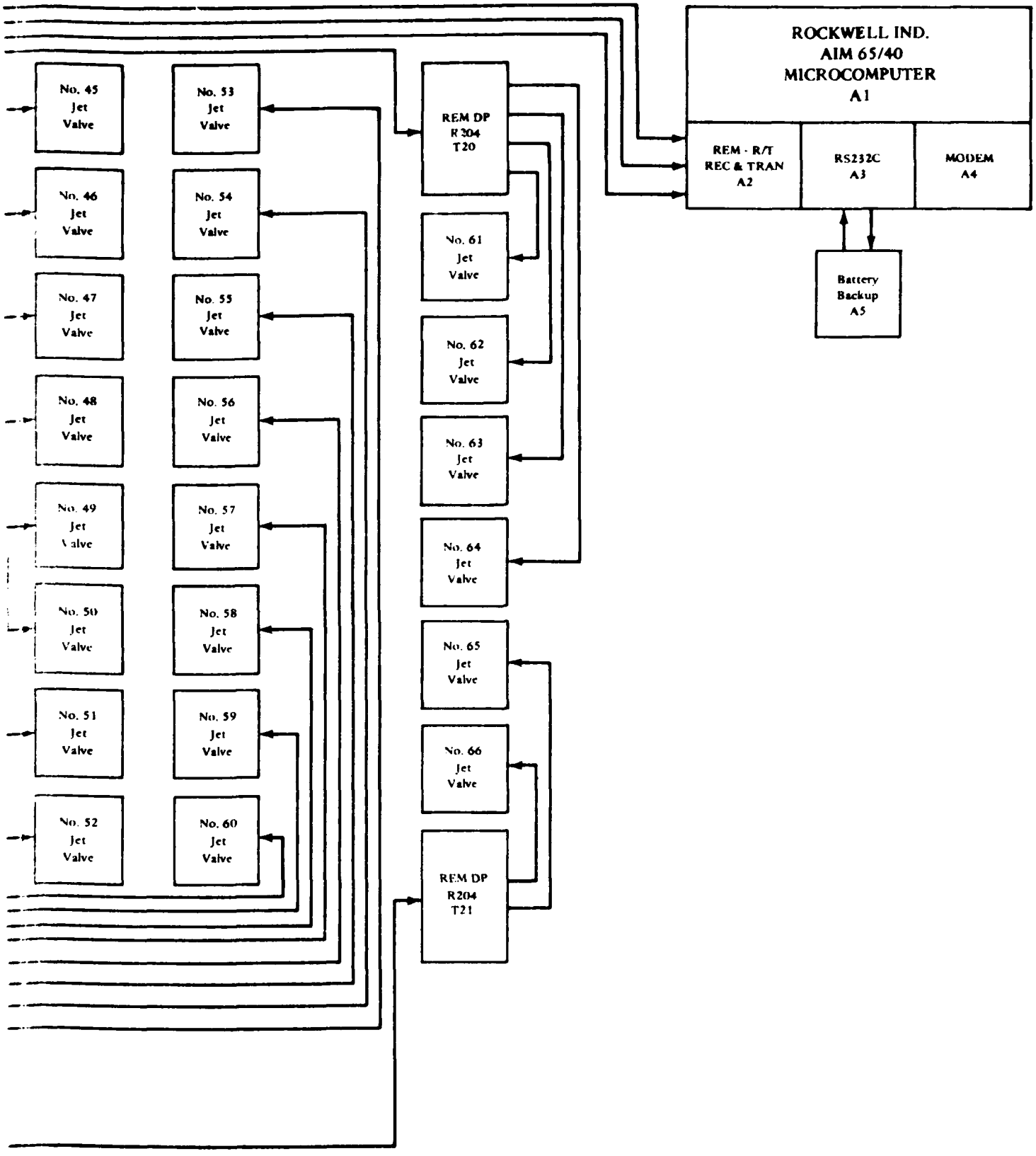
ROCKWELL IND.
AIM 65/40
MICROCOMPUTER
A1
REM - R/T
REC & TRAN
A2
RS232C
A3
MODEM
A4
Battery
Backup
A5
REM DP
R304
T20
REM DP
R204
T21
No. 45 Jet Valve
No. 46 Jet Valve
No. 47 Jet Valve
No. 48 Jet Valve
No. 49 Jet Valve
No. 50 Jet Valve
No. 51 Jet Valve
No. 52 Jet Valve
No. 53 Jet Valve
No. 54 Jet Valve
No. 55 Jet Valve
No. 56 Jet Valve
No. 57 Jet Valve
No. 58 Jet Valve
No. 59 Jet Valve
No. 60 Jet Valve
No. 61 Jet Valve
No. 62 Jet Valve
No. 63 Jet Valve
No. 64 Jet Valve
No. 65 Jet Valve
No. 66 Jet Valve

ROICC Key West FL; ROICC, Diego Garcia Island; ROICC, Keflavik, Iceland; ROICC, NAS, Corpus Christi, TX; ROICC, Pacific, San Bruno CA; ROICC, Yap; ROICC-OICC-SPA, Norfolk, VA
NAVFORCARIB Commander (N42), Puerto Rico
NAVMAG PWD - Engr Div, Guam; SCE, Subic Bay, R.P.
NAVOCEANO Code 3432 (J. DePalma), Bay St. Louis MS; Library Bay St. Louis, MS
NAVOCEANSYSCEN Code 4473 Bayside Library, San Diego, CA; Code 4473B (Tech Lib) San Diego, CA; Code 09 (Talkington), San Diego, CA; Code 5204 (J. Stachiw), San Diego, CA; Code 5214 (H. Wheeler), San Diego CA; Code 5221 (R.Jones) San Diego Ca; Code 5322 (Bachman) San Diego, CA; Hawaii Lab (R Yumori) Kailua, HI; Hi Lab Tech Lib Kailua HI
NAVORDSTA PWO, Louisville KY
NAVPETOFF Code 30, Alexandria VA
NAVPETRES Director, Washington DC
NAVPGSCOL C. Morers Monterey CA; Code 61WL (O. Wilson) Monterey CA; E. Thornton, Monterey CA
NAVPHIBASE CO, ACB 2 Norfolk, VA; Code S3T, Norfolk VA; Harbor Clearance Unit Two, Little Creek, VA; SCE Coronado, SD,CA
NAVREGMEDCEN Code 29, Env. Health Serv, (Al Bryson) San Diego, CA; PWD - Engr Div, Camp Lejeune, NC; PWO, Camp Lejeune, NC
NAVREGMEDCEN PWO, Okinawa, Japan
NAVREGMEDCEN SCE; SCE San Diego, CA; SCE, Camp Pendleton CA; SCE, Guam; SCE, Newport, RI; SCE, Oakland CA
NAVREGMEDCEN SCE, Yokosuka, Japan
NAVREGMEDCLINIC A. Watanabe, Pearl Harbor, HI
NAVSCOLCECOFF C35 Port Hueneme, CA; CO, Code C44A Port Hueneme, CA
NAVSCSOL PWO, Athens GA
NAVSEASYSCOM Code SEA OOC Washington, DC; SEA 04E (L Kess) Washington, DC; SEA05E1, Washington, D.C.
NAVSECGRUACT PWO, Adak AK; PWO, Edzell Scotland; PWO, Puerto Rico; PWO, Torri Sta, Okinawa
NAVSECSTA PWD - Engr Div, Wash., DC
NAVSHIPREPFAC Library, Guam; SCE Subic Bay
NAVSHIPYD Bremerton, WA (Carr Inlet Acoustic Range); Code 134, Pearl Harbor, HI; Code 202.4, Long Beach CA; Code 202.5 (Library) Puget Sound, Bremerton WA; Code 380, Portsmouth, VA; Code 400, Puget Sound; Code 410, Mare Is., Vallejo CA; Code 440 Portsmouth NH; Code 440, Norfolk; Code 440, Puget Sound, Bremerton WA; L.D. Vivian; Library, Portsmouth NH; PW Dept, Long Beach, CA; PWD (Code 420) Dir Portsmouth, VA; PWD (Code 450-HD) Portsmouth, VA; PWD (Code 457-HD) Shop 07, Portsmouth, VA; PWD (Code 460) Portsmouth, VA; PWO, Bremerton, WA; PWO, Mare Is.; PWO, Puget Sound; SCE, Pearl Harbor HI; Tech Library, Vallejo, CA
NAVSTA CO Roosevelt Roads P.R. Puerto Rico; Dir Engr Div, PWD, Mayport FL; Engr. Dir., Rota Spain; Long Beach, CA; Maint. Cont. Div., Guantanamo Bay Cuba; Maint. Div. Dir/Code 531, Rodman Panama Canal; PWD (LTJG.P.M. Motolenich), Puerto Rico; PWD - Engr Dept, Adak, AK; PWD - Engr Div, Midway Is.; PWO, Guantanamo Bay Cuba; PWO, Keflavik Iceland; PWO, Mayport FL; SCE, Guam; SCE, Pearl Harbor HI; SCE, San Diego CA; SCE, Subic Bay, R.P.; Security Offr, San Francisco, CA; Utilities Engr Off, Rota Spain
NAVSUBASE SCE, Pearl Harbor HI
NAVSUPPACT PWO Naples Italy
NAVSUPPFAC PWD - Maint. Control Div, Thurmont, MD
NAVSURFWPNCEN PWO, White Oak, Silver Spring, MD
NAVTECHTRACEN SCE, Pensacola FL
NAVWPNCEN Code 24 (Dir Safe & Sec) China Lake, CA; Code 2636 China Lake; Code 3803 China Lake, CA; PWO (Code 266) China Lake, CA
NAVWPNSTA (Clebak) Colts Neck, NJ; Code 092, Colts Neck NJ; Code 092, Concord CA; Maint. Control Dir., Yorktown VA
NAVWPNSTA PW Office Yorktown, VA
NAVWPNSTA PWD - Maint Control Div, Charleston, SC; PWD - Maint. Control Div., Concord, CA; PWD - Supr Gen Engr, Seal Beach, CA; PWO, Charleston, SC; PWO, Seal Beach CA
NAVWPNSUPPCEN Code 09 Crane IN
NCBC Code 10 Davisville, RI; Code 15, Port Hueneme CA; Code 156, Port Hueneme, CA; Code 25111 Port Hueneme, CA; Code 400, Gulfport MS; Code 430 (PW Engrng) Gulfport, MS; Code 470.2, Gulfport, MS; NEESA Code 252 (P Winters) Port Hueneme, CA; PWO (Code 80) Port Hueneme, CA; PWO, Davisville RI; PWO, Gulfport, MS
NCR 20, Code R70; 20, Commander
NMCB FIVE, Operations Dept; Forty, CO; THREE, Operations Off.
NOAA (Dr. T. Mc Guinness) Rockville, MD; Library Rockville, MD
NORDA Code 410 Bay St. Louis, MS; Code 440 (Ocean Rsch Off) Bay St. Louis MS
NRL Code 5800 Washington, DC; Code 5843 (F. Rosenthal) Washington, DC; Code 8441 (R.A. Skop), Washington DC
NROTC J.W. Stephenson, UC, Berkeley, CA

NSC CO, Biomedical Rsch Lab, Oakland CA; Code 44 (Security Officer) Oakland, CA; Code 54.1 Norfolk, VA; Security Offr, Hawaii
NSD SCE, Subic Bay, R.P.
NSWSES Code 0150 Port Hueneme, CA
NUCLEAR REGULATORY COMMISSION T.C. Johnson, Washington, DC
NUSC Code 131 New London, CT; Code 332, B-80 (J. Wilcox) New London, CT; Code 5202 (S. Schady) New London, CT; Code EA123 (R.S. Munn), New London CT; Code SB 331 (Brown), Newport RI; Code TA131 (G. De la Cruz), New London CT
ONR Central Regional Office, Boston, MA; Code 481, Bay St. Louis, MS; Code 485 (Silva) Arlington, VA; Code 700F Arlington VA
PACMISRANFAC HI Area Bkg Sands, PWO Kekaha, Kauai, HI
PHIBCB 1 P&E, San Diego, CA
PMTC EOD Mobile Unit, Point Mugu, CA
PWC CO Norfolk, VA; CO, (Code 10), Oakland, CA; CO, Great Lakes IL; CO, Pearl Harbor HI; Code 10, Great Lakes, IL; Code 105 Oakland, CA; Code 110, Oakland, CA; Code 120, Oakland CA; Library, Code 120C, San Diego, CA; Code 128, Guam; Code 154 (Library), Great Lakes, IL; Code 200, Great Lakes IL; Code 200, Guam; Code 30V, Norfolk, VA; Code 400, Great Lakes, IL; Code 400, Oakland, CA; Code 400, Pearl Harbor, HI; Code 400, San Diego, CA; Code 420, Great Lakes, IL; Code 420, Oakland, CA; Code 424, Norfolk, VA; Code 500 Norfolk, VA; Code 505A Oakland, CA; Code 600, Great Lakes, IL; Code 610, San Diego Ca; Code 700, Great Lakes, IL; Code 700, San Diego, CA; Library, Guam; Library, Norfolk, VA; Library, Oakland, CA; Library, Pearl Harbor, HI; Library, Pensacola, FL; Library, Subic Bay, R.P.; Library, Yokosuka JA; Util Dept (R Pascua) Pearl Harbor, HI; Utilities Officer, Guam
SPCC PWO (Code 120) Mechanicsburg PA
SUPANX PWO, Williamsburg VA
TVA Solar Group, Arnold, Knoxville, TN
UCT ONE OIC, Norfolk, VA
UCT TWO OIC, Port Hueneme CA
US DEPT OF HEALTH, ED., & WELFARE Food & Drug Admin, (A. Story), Dauphin Is, AL
US DEPT OF INTERIOR Bur of Land Mgmnt Code 583, Washington DC
US GEOLOGICAL SURVEY Off, Marine Geology, Piteleki, Reston VA
USAF REGIONAL HOSPITAL Fairchild AFB, WA
USCG (G-MP-3/USP/82) Washington Dc; (Smith), Washington, DC; G-EOE-4 (T Dowd), Washington, DC
USCG R&D CENTER CO Groton, CT; D. Motherway, Groton CT
USDA Forest Products Lab, Madison WI; Forest Products Lab, (R. DeGroot), Madison WI; Forest Service Reg 3 (R. Brown) Albuquerque, NM; Forest Service, Bowers, Atlanta, GA; Forest Service, San Dimas, CA
USNA ENGRNG Div, PWD, Annapolis MD; Energy-Environ Study Grp, Annapolis, MD; Environ, Prot, R&D Prog, (J. Williams), Annapolis MD; USNA/Sys Eng Dept, Annapolis, MD; PWO Annapolis MD
USS FULTON WPNS Rep, Offr (W-3) New York, NY
USS HOLLAND Repair Officer, New York, NY
WATER & POWER RESOURCES SERVICE (Smoak) Denver, CO
BROOKHAVEN NATL LAB M. Steinberg, Upton NY
GEORGIA INSTITUTE OF TECHNOLOGY (LT R. Johnson) Atlanta, GA

ROICC Key West FL; ROICC, Diego Garcia Island; ROICC, Keflavik, Iceland; ROICC, NAS, Corpus Christi, TX; ROICC, Pacific, San Bruno CA; ROICC, Yap; ROICC-OICC-SPA, Norfolk, VA

NAVFORCARIB Commander (N42), Puerto Rico

NAVMAG PWD - Engr Div, Guam; SCE, Subic Bay, R.P.

NAVOCEANO Code 3432 (J. DePalma), Bay St. Louis MS; Library Bay St. Louis, MS

NAVOCEANSYSCEN Code 4473 Bayside Library, San Diego, CA; Code 4473B (Tech Lib) San Diego, CA; Code 09 (Talkington), San Diego, CA; Code 5204 (J. Stachiw), San Diego, CA; Code 5214 (H. Wheeler), San Diego CA; Code 5221 (R.Jones) San Diego Ca; Code 5322 (Bachman) San Diego, CA; Hawaii Lab (R Yumori) Kailua, HI; Hi Lab Tech Lib Kailua HI

NAVORDSTA PWO, Louisville KY

NAVPETOFF Code 30, Alexandria VA

NAVPETRES Director, Washington DC

NAVPGSCOL C. Morers Monterey CA; Code 61WL (O. Wilson) Monterey CA; E. Thornton, Monterey CA

NAVPHIBASE CO, ACB 2 Norfolk, VA; Code S3T, Norfolk VA; Harbor Clearance Unit Two, Little Creek, VA; SCE Coronado, SD,CA

NAVREGMEDCEN Code 29, Env. Health Serv. (Al Bryson) San Diego, CA; PWD - Engr Div, Camp Lejeune, NC; PWO, Camp Lejeune, NC

NAVREGMEDCEN PWO, Okinawa, Japan

NAVREGMEDCEN SCE; SCE San Diego, CA; SCE, Camp Pendleton CA; SCE, Guam; SCE, Newport, RI; SCE, Oakland CA

NAVREGMEDCEN SCE, Yokosuka, Japan

NAVREGMEDCLINIC A. Watanabe, Pearl Harbor, HI

NAVSCOLCECOFF C35 Port Hueneme, CA; CO, Code C44A Port Hueneme, CA

NAVSCSOL PWO, Athens GA

NAVSEASYSCOM Code SEA OOC Washington, DC; SEA 04E (L Kess) Washington, DC; SEA05E1, Washington, D.C.

NAVSECGRUACT PWO, Adak AK; PWO, Edzell Scotland; PWO, Puerto Rico; PWO, Torri Sta, Okinawa

NAVSECSTA PWD - Engr Div, Wash., DC

NAVSHIPREPFAC Library, Guam; SCE Subic Bay

NAVSHIPYD Bremerton, WA (Carr Inlet Acoustic Range); Code 134, Pearl Harbor, HI; Code 202.4, Long Beach CA; Code 202.5 (Library) Puget Sound, Bremerton WA; Code 380, Portsmouth, VA; Code 400, Puget Sound; Code 410, Mare Is., Vallejo CA; Code 440 Portsmouth NH; Code 440, Norfolk; Code 440, Puget Sound, Bremerton WA; L.D. Vivian; Library, Portsmouth NH; PW Dept, Long Beach, CA; PWD (Code 420) Dir Portsmouth, VA; PWD (Code 450-HD) Portsmouth, VA; PWD (Code 457-HD) Shop 07, Portsmouth, VA; PWD (Code 460) Portsmouth, VA; PWO, Bremerton, WA; PWO, Mare Is.; PWO, Puget Sound; SCE, Pearl Harbor HI; Tech Library, Vallejo, CA

NAVSTA CO Roosevelt Roads P.R. Puerto Rico; Dir Engr Div, PWD, Mayport FL; Engr. Dir., Rota Spain; Long Beach, CA; Maint. Cont. Div., Guantanamo Bay Cuba; Maint. Div. Dir/Code 531, Rodman Panama Canal; PWD (LTJG.P.M. Motolenich), Puerto Rico; PWD - Engr Dept, Adak, AK; PWD - Engr Div, Midway Is.; PWO, Guantanamo Bay Cuba; PWO, Keflavik Iceland; PWO, Mayport FL; SCE, Guam; SCE, Pearl Harbor HI; SCE, San Diego CA; SCE, Subic Bay, R.P.; Security Offr, San Francisco, CA; Utilities Engr Off, Rota Spain

NAVSUBASE SCE, Pearl Harbor HI

NAVSUPPACT PWO Naples Italy

NAVSUPPFAC PWD - Maint. Control Div, Thurmont, MD

NAVSURFWPNCEN PWO, White Oak, Silver Spring, MD

NAVTECHTRACEN SCE, Pensacola FL

NAVWPNCEN Code 24 (Dir Safe & Sec) China Lake, CA; Code 2636 China Lake; Code 3803 China Lake, CA; PWO (Code 266) China Lake, CA

NAVWPNSTA (Clebak) Colts Neck, NJ; Code 092, Colts Neck NJ; Code 092, Concord CA; Maint. Control Dir., Yorktown VA

NAVWPNSTA PW Office Yorktown, VA

NAVWPNSTA PWD - Maint Control Div, Charleston, SC; PWD - Maint. Control Div., Concord, CA; PWD - Supr Gen Engr, Seal Beach, CA; PWO, Charleston, SC; PWO, Seal Beach CA

NAVWPNSUPPCEN Code 09 Crane IN

NCBC Code 10 Davisville, RI; Code 15, Port Hueneme CA; Code 156, Port Hueneme, CA; Code 25111 Port Hueneme, CA; Code 400, Gulfport MS; Code 430 (PW Engrng) Gulfport, MS; Code 470.2, Gulfport, MS; NEESA Code 252 (P Winters) Port Hueneme, CA; PWO (Code 80) Port Hueneme, CA; PWO, Davisville RI; PWO, Gulfport, MS

NCR 20, Code R70; 20, Commander

NMCB FIVE, Operations Dept; Forty, CO; THREE, Operations Off.

NOAA (Dr. T. Mc Guinness) Rockville, MD; Library Rockville, MD

NORDA Code 410 Bay St. Louis, MS; Code 440 (Ocean Rsch Off) Bay St. Louis MS

NRL Code 5800 Washington, DC; Code 5843 (F. Rosenthal) Washington, DC; Code 8441 (R.A. Skop), Washington DC

NROTC J.W. Stephenson, UC, Berkeley, CA

NSC CO, Biomedical Rsch Lab, Oakland CA; Code 44 (Security Officer) Oakland, CA; Code 54.1 Norfolk, VA; Security Offr, Hawaii
NSD SCE, Subic Bay, R.P.
NSWSES Code 0150 Port Hueneme, CA
NUCLEAR REGULATORY COMMISSION T.C. Johnson, Washington, DC
NUSC Code 131 New London, CT; Code 332, B-80 (J. Wilcox) New London, CT; Code 5202 (S. Schady) New London, CT; Code EA123 (R.S. Munn), New London CT; Code SB 331 (Brown), Newport RI; Code TA131 (G. De la Cruz), New London CT
ONR Central Regional Office, Boston, MA; Code 481, Bay St. Louis, MS; Code 485 (Silva) Arlington, VA; Code 700F Arlington VA
PACMISRANFAC HI Area Bkg Sands, PWO Kekaha, Kauai, HI
PHIBCB 1 P&E, San Diego, CA
PMTC EOD Mobile Unit, Point Mugu, CA
PWC CO Norfolk, VA; CO, (Code 10), Oakland, CA; CO, Great Lakes IL; CO, Pearl Harbor HI; Code 10, Great Lakes, IL; Code 105 Oakland, CA; Code 110, Oakland, CA; Code 120, Oakland CA; Library, Code 120C, San Diego, CA; Code 128, Guam; Code 154 (Library), Great Lakes, IL; Code 200, Great Lakes IL; Code 200, Guam; Code 30V, Norfolk, VA; Code 400, Great Lakes, IL; Code 400, Oakland, CA; Code 400, Pearl Harbor, HI; Code 400, San Diego, CA; Code 420, Great Lakes, IL; Code 420, Oakland, CA; Code 424, Norfolk, VA; Code 500 Norfolk, VA; Code 505A Oakland, CA; Code 600, Great Lakes, IL; Code 610, San Diego Ca; Code 700, Great Lakes, IL; Code 700, San Diego, CA; Library, Guam; Library, Norfolk, VA; Library, Oakland, CA; Library, Pearl Harbor, HI; Library, Pensacola, FL; Library, Subic Bay, R.P.; Library, Yokosuka JA; Util Dept (R Pascua) Pearl Harbor, HI; Utilities Officer, Guam
SPCC PWO (Code 120) Mechanicsburg PA
SUPANX PWO, Williamsburg VA
TVA Solar Group, Arnold, Knoxville, TN
UCT ONE OIC, Norfolk, VA
UCT TWO OIC, Port Hueneme CA
US DEPT OF HEALTH, ED., & WELFARE Food & Drug Admin, (A. Story), Dauphin Is, AL
US DEPT OF INTERIOR Bur of Land Mgmnt Code 583, Washington DC
US GEOLOGICAL SURVEY Off. Marine Geology, Piteleki, Reston VA
USAF REGIONAL HOSPITAL Fairchild AFB, WA
USCG (G-MP-3/USP/82) Washington Dc; (Smith), Washington, DC; G-EOE-4 (T Dowd), Washington, DC
USCG R&D CENTER CO Groton, CT; D. Motherway, Groton CT
USDA Forest Products Lab, Madison WI; Forest Products Lab. (R. DeGroot), Madison WI; Forest Service Reg 3 (R. Brown) Albuquerque, NM; Forest Service, Bowers, Atlanta, GA; Forest Service, San Dimas, CA
USNA ENGRNG Div, PWD, Annapolis MD; Energy-Environ Study Grp, Annapolis, MD; Environ. Prot. R&D Prog. (J. Williams), Annapolis MD; USNA/Sys Eng Dept, Annapolis, MD; PWO Annapolis MD
USS FULTON WPNS Rep. Offr (W-3) New York, NY
USS HOLLAND Repair Officer, New York, NY
WATER & POWER RESOURCES SERVICE (Smoak) Denver, CO
BROOKHAVEN NATL LAB M. Steinberg, Upton NY
GEORGIA INSTITUTE OF TECHNOLOGY (LT R. Johnson) Atlanta, GA

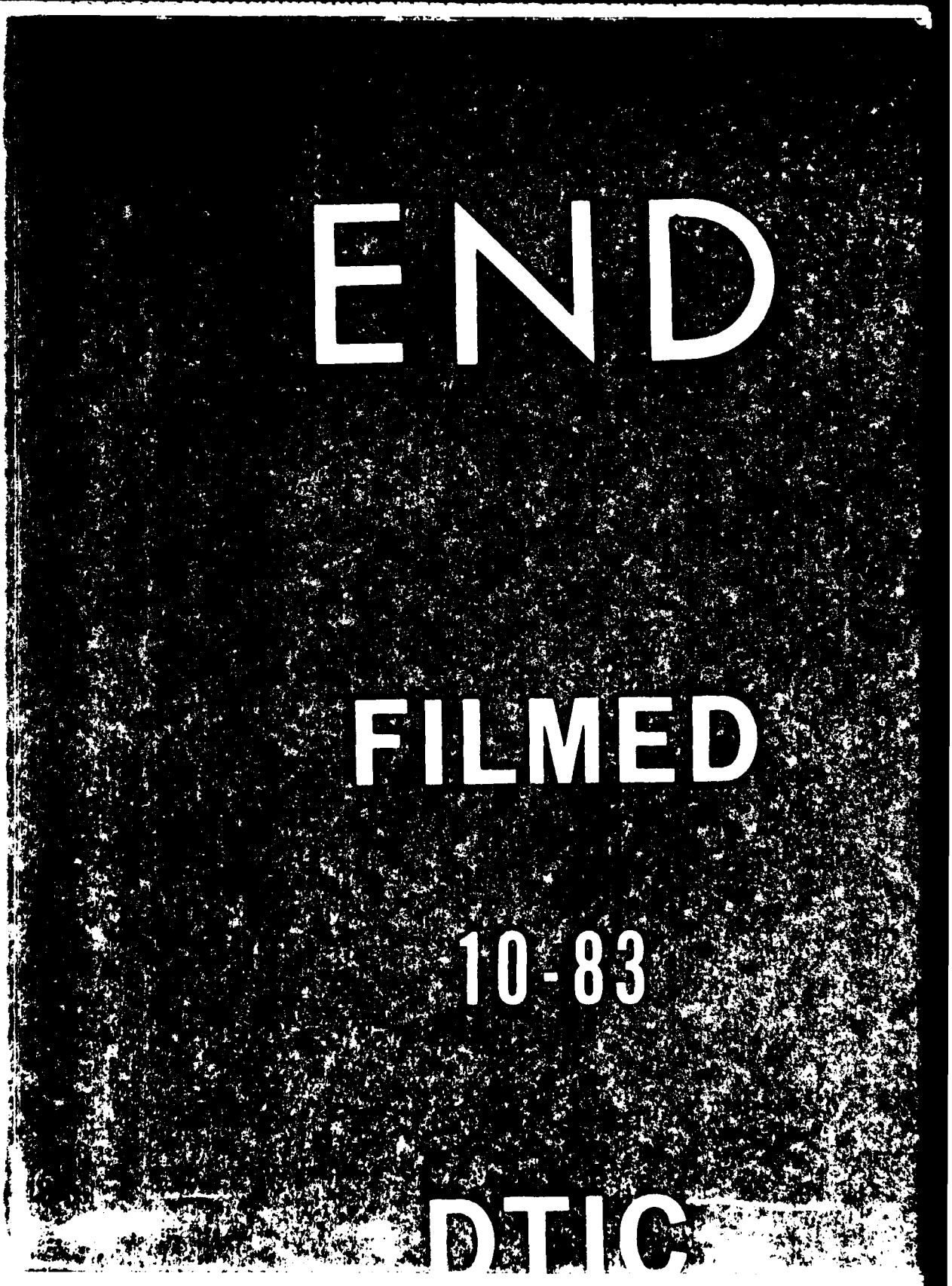
END
FILMED
10-83
DTIC